SUPPLEMENTARY MATERIALS

SUPPLEMENTARY METHODS

1.1 Biological material – cell cultures and environmental samples

To assess the composition of various birefringent cell inclusions among microscopic eukaryotes, we screened species from environmental samples, cell cultures obtained from various culture collections, and strains from private collections that were kindly donated by our collaborators (listed in Table S1 and acknowledgements). The cultivation conditions for each of the tested species are shown in Table S1. Environmental samples were assessed within one week after collection. Cell cultures were observed after transfer to fresh media on the same day and/or during five consecutive days until the purine inclusions were observed. In some cases (marked with "*" in Table S1), we transferred the cells to media containing dissolved guanine (approximately 30 μM final concentration), in order to facilitate the formation of crystalline inclusions.

1.2 Polarization microscopy

We used polarization microscopy to screen organisms for intracellular crystalline inclusions. Initially, polarization microscopy was performed separately, using an Olympus AX 70 Provis microscope (Olympus, Japan) or confocal microscope (Leica TCS SP8; Leica, Germany) equipped with a digital camera (Leica MC170 HD; Leica, Germany). After installing the polarization filters directly on the Raman microscope (WITec alpha300 RSA, WITec, Germany), photomicrographs and videos were taken immediately before Raman measurements. Short videos were taken using the default settings (25 fps using the Leica TCS SP8 or 20 fps using the WITec alpha300 RSA). Videos were processed using Vegas Pro 14.0 software (MAGIX, Germany).

1.3 Raman microscopy

Measurements and data-processing were performed as described elsewhere [1–3]. The advantages and possible drawbacks of this method have recently been discussed [4]. In brief, Raman map scanning of 203 species comprising more than 3 000 measurements of whole cells, and/or single spectra of crystalline inclusions of mobile cells, or cells with fast-moving cytoplasm, was done using a confocal Raman microscope (WITec alpha300 RSA) equipped with the following

objectives: 20× EC Epiplan, NA = 0.4 (Zeiss, Germany), 50× EC Epiplan-Neofluar, NA = 0.55 (Zeiss, Germany), 60× water-immersion UPlanSApo, NA 1.2 (Olympus, Japan), 100× oil-immersion UPlanFLN, NA 1.3 (Olympus, Japan). A 532 nm laser with a power of approximately 20 mW at the focal plane was used.

For Raman map scanning, cell cultures were used as follows: 1 ml of culture was centrifuged at 2000 g for 1 min, when necessary for fast-moving flagellates, immobilization was accomplished by mixing 5 µl of the cell pellet with 5 µl of 1% low-temperature-melting agarose spread under a 20 mm diameter, 0.18mm-thick quartz coverslip sealed with CoverGrip (Biotium, USA). In cases of environmental samples, where assessment of cell movement is crucial for reliable identification of species (mostly Amoebozoa and Excavata), immobilization was not used, and data acquisition was performed *via* Raman single-spectrum mode with an integration time of 0.5 s and 20 accumulations using one of the following objectives: 50× EC Epiplan- Neofluar, 60× UPlanSApo, and 100× UPlanFLN. Raman map measurements were performed with a scanning step of 200 nm in the both directions, voxel size 1 μm^3 and an integration time of 0.07 s per voxel with either the 60× UPlanSApo or 100× UPlanFLN objectives. On average, we measured 3–10 cells of each strain from each cell culture. In case of environmental samples, we measured at least one cell. Standards of pure chemical substances were measured in water suspension. To prepare the matching references for biogenic crystals of uric acid, guanine monohydrate, xanthine, and their mixtures, the substances were dissolved in an aqueous solution (4 %) of dimethylamine (DMA) and dried on the quartz slide to allow recrystallization.

Data was analyzed using WITec Project FIVE Plus v5.1 software (WITec, Germany) to implement the following steps: cosmic ray removal, background subtraction, cropping of the spectral edges affected by detector margins, spectral unmixing with the true component analysis tool, and averaging of the mean spectrum, summarizing multiple measurements in order to optimize the signal-to-noise ratio for each single spectrum of the crystalline inclusions.

1.4 Phylogenetic analyses

In an attempt to evaluate the role of nucleobase-cation symporter 1 (NCS1), nucleobase-ascorbate transporter (NAT), AzgA, and hypoxanthine-guanine phosphoribosyl transferase (HGPT) in purine crystal biocrystallization, we tested their phylogenetic distribution and the robustness of the phylogenetic placements using methods of molecular phylogenetics. We performed an extensive set of searches of eukaryotic and prokaryotic sequence databases. Using several representative sequences of each gene as queries, we performed a BLASTp search against 87 high-quality, well-annotated eukaryotic and prokaryotic genomes and transcriptomes. To

exclude the possibility that absence of NCS1, NAT, and AzgA gene in predicted proteomes from Heterolobosea, Ciliophora, and Apicomplexa is caused by suboptimal protein prediction, we also checked the presence of their homologs (using TBLASTN search) in contigs from eight nucleotide genome assemblies representing the three groups. While HGPT homologs were easy to detect, TBLASTN did not detect any purine transporter genes. Thus, we can be confident that the absence of these genes in genomic data is not artificial. Datasets containing original sequences and their manually curated homologs, identified by BLASTp search, were included into initial datasets and aligned by MAFFT version 7. These alignments were used as inputs to build Hidden Markov Models for a final sensitive homolog search by HMMER3 software [5] to identify candidate proteins from 742 eukaryotic genomes and transcriptomes included in the EukProt database of genome-scale predicted proteins across the diversity of eukaryotes [6]. To avoid bias introduced by contaminations or erroneous protein predictions in the EukProt database, we performed a preliminary set of Maximum-Likelihood phylogenetic analyses using IQ-TREE multicore version 1.6.10 [7] under LG4X model. Between every round, we manually inspected each tree to identify possible eukaryotic and prokaryotic contaminations. Suspicious sequences were used as queries against the NCBI database of non-redundant proteins (nr) and best blast hits were added to the dataset. Final gene datasets, free of contaminant sequences and in-paralogs (recent gene duplications that resulted in several homologs with almost identical sequence), were aligned by MAFFT [8]. Alignments were manually edited in BioEdit [9], phylogenetic trees were constructed by the maximum likelihood method using RAxML [10], with LG+GAMMA+F model selected by Modelgenerator [11], and 200 nonparametric bootstrap analyses. Trimmed datasets of AzgA, NCS1, NCS2, NATs, and HGPRT protein families are stored on an online depository server, which will be accessible upon full article publication: https://figshare.com/s/ec36ff8263c1114d547a.

For assessing the distribution of equilibrative nucleoside transporter or solute carrier 29 (ENT, SLC29) and concentrative nucleoside transporter (CNT, SLC28), we used seed-sequences according to the references [12] as initial datasets aligned by MAFFT version 7. These alignments were used as inputs to build a profile HMM followed by an HMM search against 57 sequences of genomes using HMMER3 software [5].

Data and materials availability: All data is available in the main text or the supplementary materials.

SUPPLEMENTARY TEXT

Results

Here we provide a detailed description of the results presented in Fig. 1 and Table S1. We examined representatives of all currently recognized eukaryotic supergroups [13, 14] for the presence and composition of various biocrystals. Out of the 205 observed samples, 80 % contained light-polarizing structures (Movie 1–8) that we further identified to be different inclusions, among which 95 % happened to be crystalline inclusions with 80% proportion of purines. In total, crystalline inclusions were found in 77 % of measured cell cultures or environmental samples that were equally proportional in the dataset. With the focus on purine inclusions, we found anhydrous guanine, guanine monohydrate, uric acid and xanthine. To the best of our knowledge, this is the first report on the occurrence of pure crystalline guanine monohydrate in any microorganism. Apart from purine inclusions being formed by pure substances (Fig. S1), we also found four species forming mixed crystals consisting of various proportions of guanine monohydrate, uric acid and/or xanthine (Fig. S2).

Guanine inclusions (Movie S1) were ubiquitous within the **SAR** clade (Stramenopiles, Alveolata, Rhizaria). In **Alveolata,** we confirmed, for the first time, that the morphologically prominent "polar granules" in unsporulated oocysts of the parasitic apicomplexan *Eimeria maxima* consist of guanine. Furthermore, we proved that inclusions in all observed alveolates, including parasitic apicomplexans (*Eimeria maxima*, *Psychodiella sergenti*), photoparasitic chromerids, and very diversified and ecologically important dinoflagellates and ciliates consist exclusively of guanine. Among dinoflagellates, our sampling included clades with species having plastids derived from diatoms (*Glenodinium foliaceum*) and also those having complex plastids of rhodophyte origin. Moreover, we also included the bloom- or red-tide-causing species *Heterocapsa triquetra* and a fresh isolate of Symbiodiniaceae from the soft coral *Capnella imbricata*.

Compared to Alveolata, in **Stramenopiles** the situation is more complex. Guanine crystals predominate in most species, such as predatory actinophryids, bicosoecids, phototrophic and heterotrophic chrysophytes (*Synura hibernica*, *Spumella* sp., respectively), biotechnologically promising eustigmatophytes (*Nannochloropsis oculata, Eustigmatos* cf. *polyphem*), labyrinthulomycetes (*Schizochytrium* sp.), raphidophytes (*Gonyostomum* sp.), and xanthophytes (*Botrydiopsis intercedens*, *Tribonema aequale*, *Xanthonema* sp.). In contrast, diatoms have a lower prevalence of crystalline inclusions than other stramenopiles and exhibit production of uric acid crystals, for example freshwater species of *Encyonema*, *Fragilaria*, *Navicula*, and *Pleurosigma*. Guanine crystals were detected in only a single marine/brackish diatom species (Naviculaceae gen. sp., *Seminavis*-like). Diatoms are known for a very complex nitrogen metabolism employing a urea cycle comparable to the one in animals [15]. Crystalline inclusions

were not detected in the parasitic *Blastocystis* (Opalinata) or in Oomycota. Guanine crystals predominated in the sampled **Rhizaria** (*i.e.,* Cercozoa). In Gromiida and in Retaria (Foraminifera, Acantharea, Polycystinea) we suspected the previously described structures called “stercomata” [16] to be crystals of purines, calcite or celestite (strontium sulfate). For now, we did not prove any of those with certainty due to low sampling of only three species of formalin-fixed cells of Acantharea and Foraminifera.

The more intricate crystals of **Haptista** may contain a mixture of both purines (Movie S2). Among haptophytes, *Emiliania huxleyi*, a model organism with ecological importance, possesses guanine crystals, whereas the biotechnologically important *Isochrysis* sp. has xanthine crystals. In both cases, organisms were cultured in guanine-supplemented medium (Table 1). Centroplasthelida from freshwater habitats (*Rhaphidiophrys* sp.) possessed numerous guanine crystals. **Telonemida** (*Telonema* sp.) contained guanine inclusions when cultured in guanine-supplemented medium. Within **Cryptista (***Chroomonas* sp., *Cryptomonas* sp.) we showed that the highly refractile and taxonomically important Maupas body[17] consists of uric acid.

In **Archaeplastida** (Movie S3), guanine crystals were present in glaucophytes but were not detected in any of the nine sampled rhodophyte species. Guanine inclusions are consistently distributed throughout the UTC clade (Ulvophyceae, Chlorophyceae, and Trebouxiophyceae) except for the biotechnologically significant species, *Chlorella vulgaris*, which possess xanthine, and *Dictyosphaerium* sp. which contains uric acid crystals. The arctic species *Chloromonas arctica* possesses guanine crystals. Interestingly, *Chlamydomonas* in culture or environmental samples possesses guanine crystals in different life stages from flagellate to palmelloid. Xanthine is also present in the crystals of chlorodendrophytes, including another biotechnologically exploited species, *Tetraselmis subcordiformis*, whereas other marine chlorophyte counterparts contain guanine crystals (*e.g. Nephroselmis* sp.). The smallest free-living eukaryote, with the size of bacteria, *Ostreococcus tauri* (Mamiellophyceae), did not show any crystalline inclusions even though they may contain starch as a storage polysaccharide. It is also possible that our methods had insufficient resolution to detect crystalline inclusions in these tiny cells. In stark contrast to Chlorophyta, the Streptophyta, notably including land plants (Embryophyta) together with the related microalgae, Zygnematophyceae and Klebsormidiophyceae, contain uric acid inclusions. In the case of *Mesotaenium caldariorum*, the predominant uric acid includes admixtures of crystalline guanine monohydrate. However, other examined streptophytes such as *Chlorokybus atmophyticus* (Chlorokybophyceae) form guanine crystals. We detected no crystalline inclusions in *Mesostigma viride* (Mesostigmatophyceae). In Embryophyta, Coleochaetophyceae, and Zygnematophyceae we observed calcium oxalate inclusions instead of purine crystals.

Intriguingly, the transition of crystal composition from purines in green algae to calcium oxalate in land plants may be metabolically bridged through purine degradation [18, 19]. We also see a similar trend in Fungi, with yeasts possessing purine crystals, filamentous fungi producing calcium oxalate [20, 21], and some marine seaweeds (Phaeophyceae) lacking crystals altogether. Hence, loss of the capacity to form purine crystals may correlate with the development of multicellularity that the necessity to store nitrogen is replaced by transfer of soluble metabolites through the multicellular body [22].

Crystalline inclusions of varied chemical composition, primarily guanine and xanthine, occur commonly in **Amoebozoa** (Movie S4). Xanthine crystals, uncommon in other eukaryotes, are present in freshwater and marine *Mayorella* sp., in the facultatively parasitic model organism, *Acanthamoeba castellanii*, in the anaerobic model species *Mastigamoeba balamuthi*, and a model terrestrial slime mold, *Physarum polycephalum*. By contrast, guanine was present in a fresh isolate of another slime mold, *Fuligo septica*, a different species of Archamoebae (*Mastigella eilhardi*), and in species of the common genera *Thecamoeba*, *Vannella*, and *Difflugia*.

We showed by Raman microscopy that, in **Opisthokonta,** uric acid, rather than guanine, is a common excretory product of nitrogen metabolism (*e.g.* in nematodes). Interestingly, we noticed guanine microcrystals inside swarming acoelomate gastrotrichs (Platyzoa) in a sample from a peat bog (Movie S5). Using Raman microscopy, we also confirmed that guanine crystals serve as a refractile layer on fish scales. In Fungi (Holomycota) we found crystalline guanine in *Candida albicans*, which has been tested for uptake of different purine compounds previously [23]. However, we did not find any crystalline inclusions in *Saccharomyces cerevisiae*. We observed no crystalline inclusions in either intracellular parasites belonging to Microsporidia or in the free-living halophilic Choanoflagellata. We did not detect crystalline inclusions in the **Breviatea**, close relatives of opisthokonts.

In **Excavata** (Movie S6), the crystalline inclusions, present in all studied lineages, were exclusively composed of guanine, including: both heterotrophic (*Entosiphon* sp., *Rhabdomonas* sp.) and photosynthetic euglenids, freshwater and marine euglenids (*Euglena* sp*., Eutreptiella gymnastica,* respectively), in free-living kinetoplastids (but not in the parasites, such as trypanosomatids), in deep-sea diplonemids (*Namystinia karyoxenos, Rhynchopus* sp.), aerotolerant heteroloboseans (*Naegleria gruberi*), and strictly anaerobic metamonad symbionts of termites (*e.g. Macrotrichomonoides* sp. isolated from *Neotermes cubanus*). In the diplonemid, *Flectonema* sp., guanine monohydrate was detected in the form of pure crystals, probably monocrystals, as their Raman spectra exhibit similar variability of relative intensities when excited by polarized light to that of synthetically prepared monocrystals.

We found guanine crystals in *Gefionella okellyi*, from the phylogenetically distinct clade of **Malawimonadida**. Among the **CRuMs** group (Collodictyonida, Rigifilida, and Mantamonadida), we tested mantamonads but found no crystalline inclusions inside their cells, even after exposing them to guanine-enriched culture medium. Lastly, crystalline guanine was found in *Hemimastix kukwesjijk*, the only representative sampled from **Hemimastigophora**, a separate, deep-branching lineage, recently described as a new eukaryotic supergroup (Movie S7).

In addition to the predominant purine crystalline inclusions (80 %), there are also other types. Surprisingly, calcite (calcium carbonate – $CaCO_3$) was present in diatoms, thus, it is another independent observation of calcification in diatoms following the previous report in [24]. However, diatoms are mostly known for their frustules formed by amorphous silica (silicon dioxide – SiO_2, opal) [25]. Calcification (Fig. S3, Tab. S1) occurred in the seaweeds tested, including rhodophytes, ulvophytes and phaeophytes, indicating that this process occurs very commonly in marine environments [26]. Similarly, calcified shells of foramiferans and the calcite scales on the cell surface of the haptophytic coccolithophore *Emiliania huxleyi* also strongly polarized light [27]. Massive calcite incrustations occurred on surface of filamentous algae, *e.g. Oedogonium* sp., that has been previously described as crystal jewels in other freshwater filamentous algae [28]. We confirmed the mixture of calcium and strontium carbonates ($(Ca,Sr)CO_3$) in the green alga *Tetraselmis*, previously reported elsewhere to be amorphous, using different methodology [29].

Crystalline sulfates occurred in various species but only rarely (Fig. S4). Similarly, in the light-polarizing armor of Acantharea, we confirmed the presence of celestite (strontium sulfate – $SrSO_4$) [30, 31]. Interestingly, we found baryte (barium sulfate – $BaSO_4$) in three species of zygnematophytes (*Closterium peracerosum-strigosum-littorale* complex, *Cosmarium* sp., and *Spirogyra* sp.), for two of which it has been previously reported [32, 33]. In laboratory cultures and environmental isolates of *Saccamoeba* sp. we found an unprecedently complex spectrum corresponding to numerous crystalline inclusions lacking light-polarization features. The dominating peak at 998 cm^{-1} (Fig. S4, Tab. S1) resembles either a signal of sulfates or aromatic compounds. The rest of the spectrum also shows lipid-like organic matter; thus, the crystals may be formed by a complex mixture of lipids and sulfates.

Calcium oxalate monohydrate ($CaC_2O_4 \cdot H_2O$) crystals were restricted to closely related streptophytic algae and land plants: Coleochaetophyceae, Zygnematophyceae (*Cylindrocystis* sp.), and Embryophyta (*e.g.* plant models *Physcomitrella patens*, *Nicotiana tabacum*) together with calcium oxalate dihydrate ($CaC_2O_4 \cdot 2H_2O$) commonly found in Embryophyta (Fig. S5, Tab.

S1). In the Embryophyta, deposition of calcium oxalate is already known to occur under stress conditions [34].

Unexpected light-polarizing lipophilic inclusions unreported until now, occurred in some of examined samples. Compared to carotene crystals observed in the model plant *Arabidopsis thaliana* [35], we found possibly similar structures in aerophytic ulvophytes (*Trentepohlia* sp., *Scotinosphaera gibberosa*) and freshwater cyanobacteria (*Oscillatoria* sp.), comprising a mixture of carotenoids and lipids containing sterols and fatty acids (Fig. S6, Table S1, Movie S8). Similarly, in the green parasitic alga, *Phyllosiphon arisari* and a symbiont of lichens, *Symbiochloris tschermakiae*, their light-polarizing lipophilic crystals were a complex mixture of lipids, with a high proportion of unsaturated fatty acids in the former, and saturated fatty acids in the latter. Faintly light-polarizing lipophilic structures in amoebozoans (*Entamoeba histolytica*) resembled those mentioned above or contained a surplus of sterol compounds (*Acanthamoeba castellanii* and *Mastigamoeba balamuthi*). Some of them may be of a crystalline nature but this requires further evidence. All lipophilic light-polarizing structures tended to melt under prolonged illumination by a focused laser beam (ca 20 mW power) during the Raman measurements.

Refractile structures such as storage polysaccharides, *i.e.,* starch or chrysolaminarin [36, 37], or aerotopes, air-filled vesicles with a reflective interface inside the cells of cyanobacteria [38], might be confused with birefringent crystals. High-intensity light-polarization also occurs in the thick cellulose cell walls of ulvophytes, zygnematophytes, rhodophytes, glaucophytes and others, a phenomenon best-studied in plants [39], or in starch, a storage polysaccharide of Archaeplastida and in chrysolaminarin, storage polysaccharide of SAR (Fig. S7, Table S1).

Comments on Raman spectra analysis

In some protists, a monohydrate of guanine in crystalline form was detected (Figs. S1 and S2). To the best of our knowledge, this is the first report confirming the occurrence of crystalline guanine monohydrate in any microorganism. To date, only a β-polymorph of crystalline anhydrous guanine was detected in various organisms, including some microalgae and protists [3, 40, 41]. In *Flectonema* sp., guanine monohydrate was detected in the form of pure crystals (Fig. S1), probably monocrystals. We observed a few inclusions formed by purine mixtures, which has also been reported from *Paramecium* [41, 42]. In the case of *Mesotaenium caldariorum*, crystalline guanine monohydrate seems to be only a minor admixture in the more abundant uric acid (Fig. S2), however its presence was demonstrated by spectral similarity with synthetically prepared samples containing both uric acid and guanine monohydrate. The inverse proportion of the two

compounds has been found in *Tetraselmis subcordiformis*. *Isochrysis* sp. and *Chroomonas* sp. exhibited crystalline mixtures of xanthine and guanine monohydrate.

Comments on phylogenetic analyses

Hypoxanthine-guanine phosphoribosyl transferase (HGPT) (Fig. S8), omnipresent in eukaryotes, can also be found in Eubacteria, Archaea and, surprisingly enough, we detected HGPT homologs also in Nucleocytoviricota genomes. Because it is a relatively short and divergent protein, we were unable to resolve its detailed phylogeny. Based on previously introduced nomenclature [43], we distinguished a clade of "fungal HGPT" which is very divergent from the other "classical HGPTs". However, we were able to find homologs of "fungal HGPT" in virtually all eukaryotic supergroups.

The nucleobase cation symporter-1 (NCS1) family (Fig. S9) of secondary active transport proteins includes proteins from prokaryotes and several lineages of eukaryotes. We recovered NCS1 eukaryotic paralogs – fungal Fcy type, fungal Fur type, algal type, and plant type as previously described [44]. Besides, we also identified four as-yet-unknown eukaryotic paralogs that we marked as NCS1 A–D. Distribution of NCS1 in eukaryotes is extremely patchy as summarized on Fig. 2. We conclude that NCS1 transporter has been acquired by eukaryotes several times independently. Fungal Fcy type is present in various Fungi (Ascomycetes, Basidiomycetes, Gonapodya). Some Fungi even contain several distant paralogs of this gene (e.g. *Aspergillus* and *Candida*). Interestingly, homologs from Oomycota form a clade within fungal sequences, branching sister to *Aspergillus* sequences with full statistical support. Thus, our analysis strongly indicates lateral transfer of this gene from Fungi (supergroup Obazoa) to Oomycota (supergroup SAR). We identified fungal Fcy type of NCS1 transporter also in Ktedonobacteria (Chloroflexi) and two groups of Proteobacteria (Betaproteobacteria and Gammaproteobacteria). Bacterial homologs of fungal Fcy form a clade branching within fungal sequences but, in this case, with relatively low bootstrap support. Besides, the whole clade of fungal Fcy sequences shows strong affinity to eubacterial permeases including those from Gammaproteobacteria and Betaproteobacteria, so in this case, lateral transfer of Fcy from Fungi to Eubacteria is less convincing. We also identified an ecological relationship between eukaryotes that possess fungal Fcy gene, all of which are adapted to extract nutrients from plants. The Fur type of NCS1 is present exclusively in Basidiomycetes and Ascomycetes (Fungi). The source organism for Fur type is unclear. The algal type of NCS1 is present in *Nannochloropsis* (SAR), Rhodophyta, and Chlorophyta (Archaeplastida). It also has an uncertain origin. Plant type NCS1 was detected in Chlorophyta and Streptophyta (closely related lineages of the supergroup

Archaeplastida). Surprisingly, this gene is also present in Rhodelphidia, another deep-branching lineage of the supergroup Archaeplastida. The gene has unclear origin, although it shows affinity to Proteobacteria with low statistical support.

We also identified four novel clades of eukaryotic NCS1 transporters. One of them is present only in dinoflagellates and shows a close relationship to cytosine permease from Actinobacteria (with full bootstrap support); another is in *Chromera*, diatoms, and dinoflagellates; it shows affinity to Bacteroidetes and Planctomycetes with full bootstrap support. The other clade contains homologs from choanoflagellates, Hemimastigophora, telonemids, dinoflagellates, Chlorophyta, and malawimonadids. The phylogenetic position of *Incisomonas marina* (Stramenopiles) within choanoflagellates is probably due to contamination, also most likely in the case of *Paulinella* (Rhizaria) within Chlorophyta. Finally, two sequences from unrelated amoebozoans (*Filamoeba* and *Vermamoeba*) form a robust clade with no affinity to any other group, forming another eukaryotic NCS1 clade.

Nucleobase-Ascorbate Transporter (NAT) protein family (Fig. S10) is an extensively studied group of proteins. All bacterial NATs are H^+ symporters highly specific for either uracil or xanthine or uric acid. The fungal and plant members are H^+ symporters specific either for xanthine-uric acid, or for adenine-guanine-hypoxanthine-uracil. In contrast to the microbial and plant proteins, most functionally characterized mammalian NATs are highly specific for L-ascorbate/Na^+. However, the rSNBT1 NAT transporter from a rat is specific for nucleobases [45]. Our analysis convincingly shows that NAT proteins were introduced to eukaryotes at least four times independently (NAT A–D) and have their closest homologs in eubacteria, NAT B and D with high statistical support. Metazoan and plant NATs both belong to the NAT A clade that is, together with NAT C, the most widespread NAT gene in eukaryotes. In contrast, NAT B is present only in Fungi and dictyostelids; NAD D is unique for *Tritrichomonas* and it was established by horizontal gene transfer from Firmicutes (it is encoded on tritrichomonas-like genomic contig, so it is not contamination). Interestingly, some well-supported eukaryotic clades are not congruent with eukaryotic phylogeny confounding interpretation of the descent of this protein family. In some cases, it might be explained by eukaryote-to-eukaryote horizontal gene transfers (*e.g.,* from fungi to dictyostelids in NAT B).

The **AzgA** gene encodes a **hypoxanthine-adenine-guanine transporter** (Fig. S11) that is present in all main groups of eukaryotes except supergroup Amoebozoa, and it is also missing in metazoans. Our analysis convincingly shows that eukaryotic AzgA has a single origin in eukaryotes and has been probably present in two paralogs in the last eukaryotic common ancestor. We

named those paralogs AzgA A and B. Besides, the analysis indicates a series of gene duplications during evolution of certain groups as seen in Chlorophyta and Dinoflagellata.

References

1. Moudříková Š, Nedbal L, Solovchenko A, Mojzeš P. Raman microscopy shows that nitrogen-rich cellular inclusions in microalgae are microcrystalline guanine. *Algal Res* 2017; **23**: 216–222.
2. Barcytė D, Pilátová J, Mojzeš P, Nedbalová L. The arctic *Cylindrocystis* (Zygnematophyceae, Streptophyta) green algae are genetically and morphologically diverse and exhibit effective accumulation of polyphosphate. *J Phycol* 2020; **56**: 217–232.
3. Mojzeš P, Gao L, Ismagulova T, Pilátová J, Moudříková Š, Gorelová O, et al. Guanine, a high-capacity and rapid-turnover nitrogen reserve in microalgal cells. *Proc Natl Acad Sci* 2020; **117**: 32722–32730.
4. Moudříková Š, Ivanov IN, Vítová M, Nedbal L, Zachleder V, Mojzeš P, et al. Comparing biochemical and Raman microscopy analyses of starch, lipids, polyphosphate, and guanine pools during the cell cycle of *Desmodesmus quadricauda*. *Cells* 2021; **10**: 1–21.
5. Eddy SR. A probabilistic model of local sequence alignment that simplifies statistical significance estimation. *PLoS Comput Biol* 2008; **4**: 1–14.
6. Richter DJ, Berney C, Strassert JFH, Burki F, de Vargas C. EukProt: A database of genome-scale predicted proteins across the diversity of eukaryotic life. *bioRxiv* 2020; 1–11.
7. Hoang DT, Chernomor O, Von Haeseler A, Minh BQ, Vinh LS. UFBoot2: Improving the ultrafast bootstrap approximation. *Mol Biol Evol* 2018; **35**: 518–522.
8. Katoh K, Standley DM. MAFFT multiple sequence alignment software version 7: Improvements in performance and usability. *Mol Biol Evol* 2013; **30**: 772–780.
9. Hall T. BioEdit: a user-friendly biological sequence alignment editor and analysis program for Windows 95/98/NT. *Nucleic Acids Symp Ser* 1999; **41**: 95–98.
10. Stamatakis A. RAxML version 8: A tool for phylogenetic analysis and post-analysis of large phylogenies. *Bioinformatics* 2014; **30**: 1312–1313.
11. Keane TM, Creevey CJ, Pentony MM, Naughton TJ, McInerney JO. Assessment of methods for amino acid matrix selection and their use on empirical data shows that ad hoc assumptions for choice of matrix are not justified. *BMC Evol Biol* 2006; **6**: 1–17.
12. Young JD, Yao SYM, Baldwin JM, Cass CE, Baldwin SA. The human concentrative and equilibrative nucleoside transporter families, SLC28 and SLC29. *Mol Aspects Med* 2013; **34**: 529–547.
13. Adl SM, Bass D, Lane CE, Lukeš J, Schoch CL, Smirnov A, et al. Revisions to the classification, nomenclature, and diversity of eukaryotes. *J Eukaryot Microbiol* 2019; **66**: 4–119.
14. Archibald JM, Simpson AGB, Slamovits CH, Margulis L, Melkonian M, Chapman DJ, et al. Handbook of the Protists, 2nd ed. *Handbook of the Protists* . 2017. Springer International Publishing, Switzerland.
15. Smith SR, Dupont CL, McCarthy JK, Broddrick JT, Oborník M, Horák A, et al. Evolution and regulation of nitrogen flux through compartmentalized metabolic networks in a marine diatom. *Nat Commun* 2019; **10**: 1–14.
16. Hedley RH, Bertaud WS. Electron-microscopic observations of *Gromia oviformis* (Sarcodina). *J Protozool* 1962; **9**: 79–87.
17. Hoef-Emden K, Melkonian M. Revision of the genus *Cryptomonas* (Cryptophyceae): A

combination of molecular phylogeny and morphology provides insights into a long-hidden dimorphism. *Protist* 2003; **154**: 371–409.
18. Brychkova G, Fluhr R, Sagi M. Formation of xanthine and the use of purine metabolites as a nitrogen source in *Arabidopsis* plants. *Plant Signal Behav* 2008; **3**: 999–1001.
19. Yu L, Jiang J, Zhang C, Jiang L, Ye N, Lu Y, et al. Glyoxylate rather than ascorbate is an efficient precursor for oxalate biosynthesis in rice. *J Exp Bot* 2010; **61**: 1625–1634.
20. Roush AH. Crystallization of purines in the vacuole of *Candida utilis*. *Nature* 1961; **190**: 449.
21. Gadd GM, Bahri-Esfahani J, Li Q, Rhee YJ, Wei Z, Fomina M, et al. Oxalate production by fungi: Significance in geomycology, biodeterioration and bioremediation. *Fungal Biol Rev* 2014; **28**: 36–55.
22. Winter G, Todd CD, Trovato M, Forlani G, Funck D. Physiological implications of arginine metabolism in plants. *Front Plant Sci* 2015; **6**: 1–14.
23. Roush AH, Questiaux LM, Domnas AJ. The active transport and metabolism of purines in the yeast, *Candida utilis*. *J Cell Comp Physiol* 1959; **54**: 275–286.
24. Ehrlich H, Motylenko M, Sundareshwar P V, Ereskovsky A, Zgłobicka I, Noga T, et al. Multiphase biomineralization: enigmatic invasive siliceous diatoms produce crystalline calcite. *Adv Funct Mater* 2016; **26**: 2503–2510.
25. Romann J, Valmalette JC, Chauton MS, Tranell G, Einarsrud MA, Vadstein O. Wavelength and orientation dependent capture of light by diatom frustule nanostructures. *Sci Rep* 2015; **5**: 1–6.
26. Lipej L, Orlando-Bonaca M, Mavrič B. Biogenic formations in the Slovenian sea. 2016.
27. Weiner S, Addadi L. Crystallization pathways in biomineralization. *Annu Rev Mater Res* 2011; **41**: 21–40.
28. Lenzenweger R. Algen mit Kristallschmuck. *Mikrokosmos* 2002; **91**: 280.
29. Martignier A, Filella M, Pollok K, Melkonian M, Bensimon M, Barja F, et al. Marine and freshwater micropearls: Biomineralization producing strontium-rich amorphous calcium carbonate inclusions is widespread in the genus *Tetraselmis* (Chlorophyta). *Biogeosciences* 2018; **15**: 6591–6605.
30. Odum HT. Notes on the strontium content of sea water, celestite Radiolaria, and strontianite snail shells. *Science* 1951; **114**: 211–213.
31. Bütschli O. Über die chemische Natur der Skelettsubstanz der Acantharia. *Zool Anz* 1906; **30**: 784–789.
32. Brook AJ, Fotheringham A, Bradly J, Jenkins A. Barium accumulation by desmids of the genus *Closterium* (Zygnemaphyceae). *Br Phycol J* 1980; **15**: 261–264.
33. Kreger DR, Boeré H. Some observations on barium sulphate in *Spirogyra*. *Acta Bot Neerl* 1969; **18**: 143–151.
34. Nakata PA. Plant calcium oxalate crystal formation, function, and its impact on human health. *Front Biol (Beijing)* 2012; **7**: 254–266.
35. Maass D, Arango J, Wüst F, Beyer P, Welsch R. Carotenoid crystal formation in *Arabidopsis* and carrot roots caused by increased phytoene synthase protein levels. *PLoS One* 2009; **4**: 1–12.
36. Xiao H, Wang S, Xu W, Yin Y, Xu D, Zhang L, et al. The study on starch granules by using darkfield and polarized light microscopy. *J Food Compos Anal* 2020; **92**: 1–7.

37. Kreger DR, van der Veer J. Paramylon in a Chrysophyte. *Acta Bot Neerl* 1970; **19**: 401–402.
38. Li J, Liao R, Tao Y, Zhuo Z, Liu Z, Deng H, et al. Probing the cyanobacterial *Microcystis* gas vesicles after static pressure treatment: A potential in situ rapid method. *Sensors* 2020; **20**: 1–17.
39. Abraham Y, Elbaum R. Quantification of microfibril angle in secondary cell walls at subcellular resolution by means of polarized light microscopy. *New Phytol* 2013; **197**: 1012–1019.
40. Jantschke A, Pinkas I, Hirsch A, Elad N, Schertel A, Addadi L, et al. Anhydrous β-guanine crystals in a marine dinoflagellate: Structure and suggested function. *J Struct Biol* 2019; **207**: 12–20.
41. Creutz CE, Mohanty S, Defalco T, Kretsinger RH. Purine composition of crystalline cytoplasmic inclusions of *Paramecium tetraurelia*. *Protist* 2002; **153**: 39–45.
42. Pinsk N, Wagner A, Cohen L, Smalley CJH, Hughes CE, Zhang G, et al. Biogenic guanine crystals are solid solutions of guanine and other purine metabolites. *J Am Chem Soc* 2022; **144**: 5180–5189.
43. Liu X, Qian W, Liu X, Qin H, Wang D. Molecular and functional analysis of hypoxanthine-guanine phosphoribosyltransferase from *Arabidopsis thaliana*. *New Phytol* 2007; **175**: 448–461.
44. Patching SG. Recent developments in nucleobase cation symporter-1 (NCS1) family transport proteins from bacteria, archaea, fungi and plants. *J Biosci* 2018; **43**: 797–815.
45. Kourkoulou A, Pittis AA, Diallinas G. Evolution of substrate specificity in the nucleobase-ascorbate transporter (NAT) protein family. *Microb Cell* 2018; **5**: 280–292.
46. Prokopchuk G, Tashyreva D, Yabuki A, Horák A, Masařová P, Lukeš J. Morphological, ultrastructural, motility and evolutionary characterization of two new Hemistasiidae species. *Protist* 2019; **170**: 259–282.
47. Bischoff HW, Bold HC. Phycological Studies IV. Some Soil Algae from Enchanted Rock and Related Algal Species. 1963. University of Texas Publication No. 6318.
48. Votýpka J, Kostygov AY, Kraeva N, Grybchuk-Ieremenko A, Tesařová M, Grybchuk D, et al. *Kentomonas* gen. n., a new genus of endosymbiont-containing trypanosomatids of Strigomonadinae subfam. n. *Protist* 2014; **165**: 825–838.
49. Andersen RA, Morton SL, Sexton JP. Provasoli Guillard National Center for Culture of Marine Phytoplankton 1997 – list of strains. *J Phycol* 1997; **33**: 1–75.
50. Guillard RRL. Culture of phytoplankton for feeding marine invertebrates. *Culture of marine invertebrate animals*. 1975. Plenum Press, New York, pp 29–60.
51. Park JS. Effects of different ion compositions on growth of obligately halophilic protozoan *Halocafeteria seosinensis*. *Extremophiles* 2012; **16**: 161–164.
52. Bertani G. Studies on lysogenesis. I. The mode of phage liberation by lysogenic Escherichia coli. *J Bacteriol* 1951; **62**: 293–300.
53. Fulton C. Axenic cultivation of *Naegleria gruberi*. Requirement for methionine. *Exp Cell Res* 1974; **88**: 365–370.
54. Samson RA, Hoekstra ES, Oorschot CAN Van. Introduction to food-borne fungi. 1981. Centraalbureau voor Schimmelcultures, Baarn et Delft, the Netherlands.
55. Murashige T, Skoog F. A revised medium for rapid growth and bio assays with tobacco

tissue cultures. *Physiol Plant* 1962; **15**: 474–497.
56. Neff RJ, Neff RH. Induction of synchronous division in amoebae. *Synchrony in Cell Division and Growth*. 1964. Wiley Interscience, New York, pp 213–246.
57. Burgess LW, Liddell CM, Summerell BA. Laboratory manual for fusarium research: incorporating a key and descriptions of common species found in Australasia, 2nd ed. 1988. The University of Sydney, Sydney, Australia.
58. Chávez LA, Balamuth W, Gong T. A light and electron microscopical study of a new, polymorphic free-living amoeba, *Phreatamoeba balamuthi* n. g., n. sp. *J Protozool* 1986; **33**: 397–404.
59. Diamond LS. Establishment of various trichomonads of animals and man in axenic cultures. *J Parasitol* 1957; **43**: 488–490.

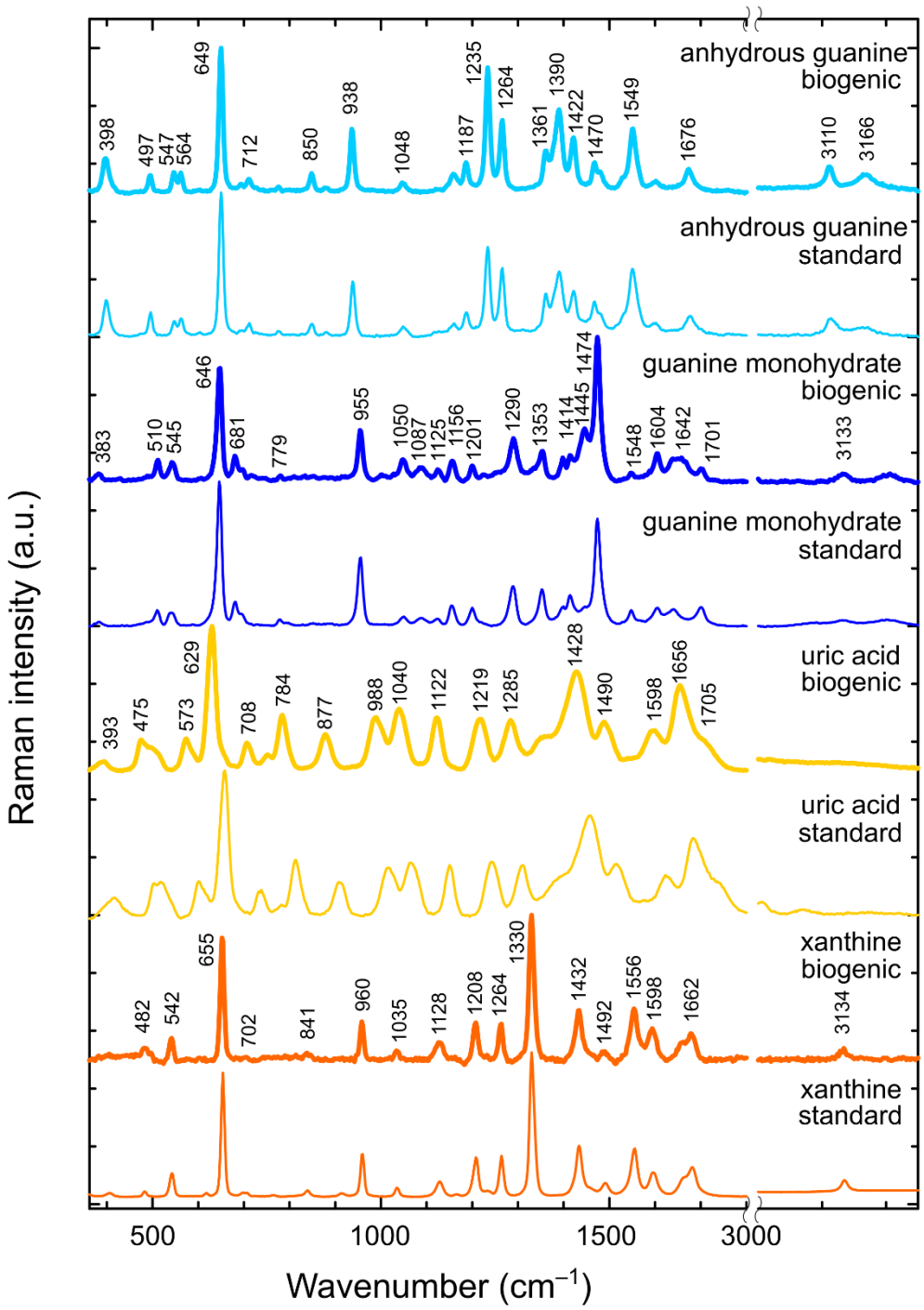

Fig. S1.

Representative Raman spectra of biogenic purine crystalline inclusions measured in biological species followed by their respective standards of pure chemical compounds. Biogenic crystals have been spectrally extracted directly from measured species. Standards of anhydrous guanine and xanthine have been measured as suspension of pure compounds in water, guanine monohydrate and uric acid has been recrystallized from 4% dimethylamine water solution.

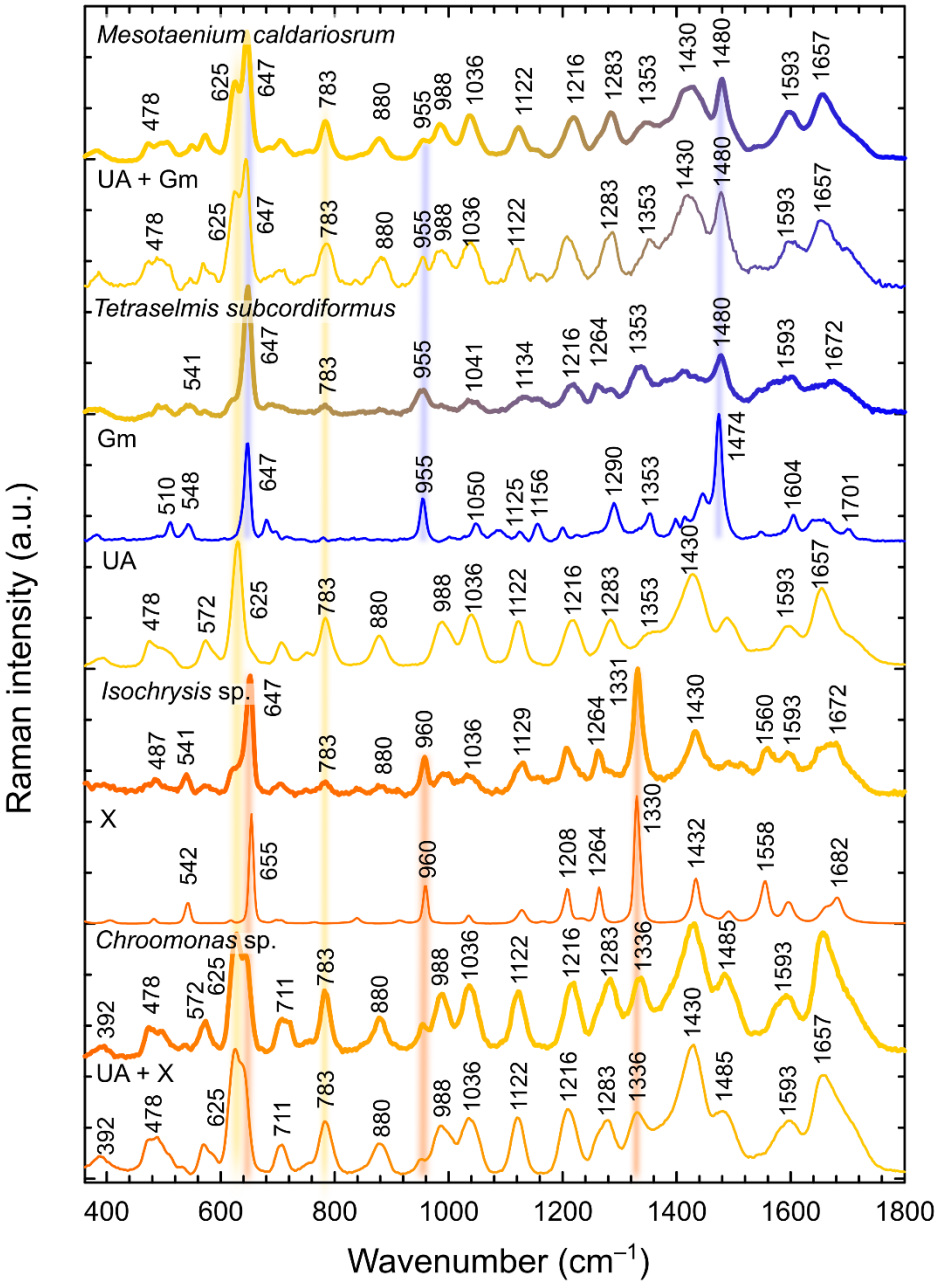

481

482 **Fig. S2.**

483 Representative Raman spectra of biogenic purine inclusions forming mixtures of uric acid (UA)
484 and guanine monohydrate (Gm) in different proportions with a dominance of the former in the
485 case of *Mesotaenium caldariorum*, or the latter in *Tetraselmis subcordiformis*. Xanthine (X)
486 dominates the crystals with uric acid admixtures found in *Isochrysis* sp., whereas *Chroomonas* sp.
487 has higher proportions of uric acid over xanthine. The reference spectra of pure substances are
488 shown along with those of mixtures of "UA + Gm" and "UA + X" recrystallized from 4%
489 dimethylamine solution, as Raman spectra of purine mixtures exhibit some spectral shifts and
490 changes in relative intensities compared to the pure substances.

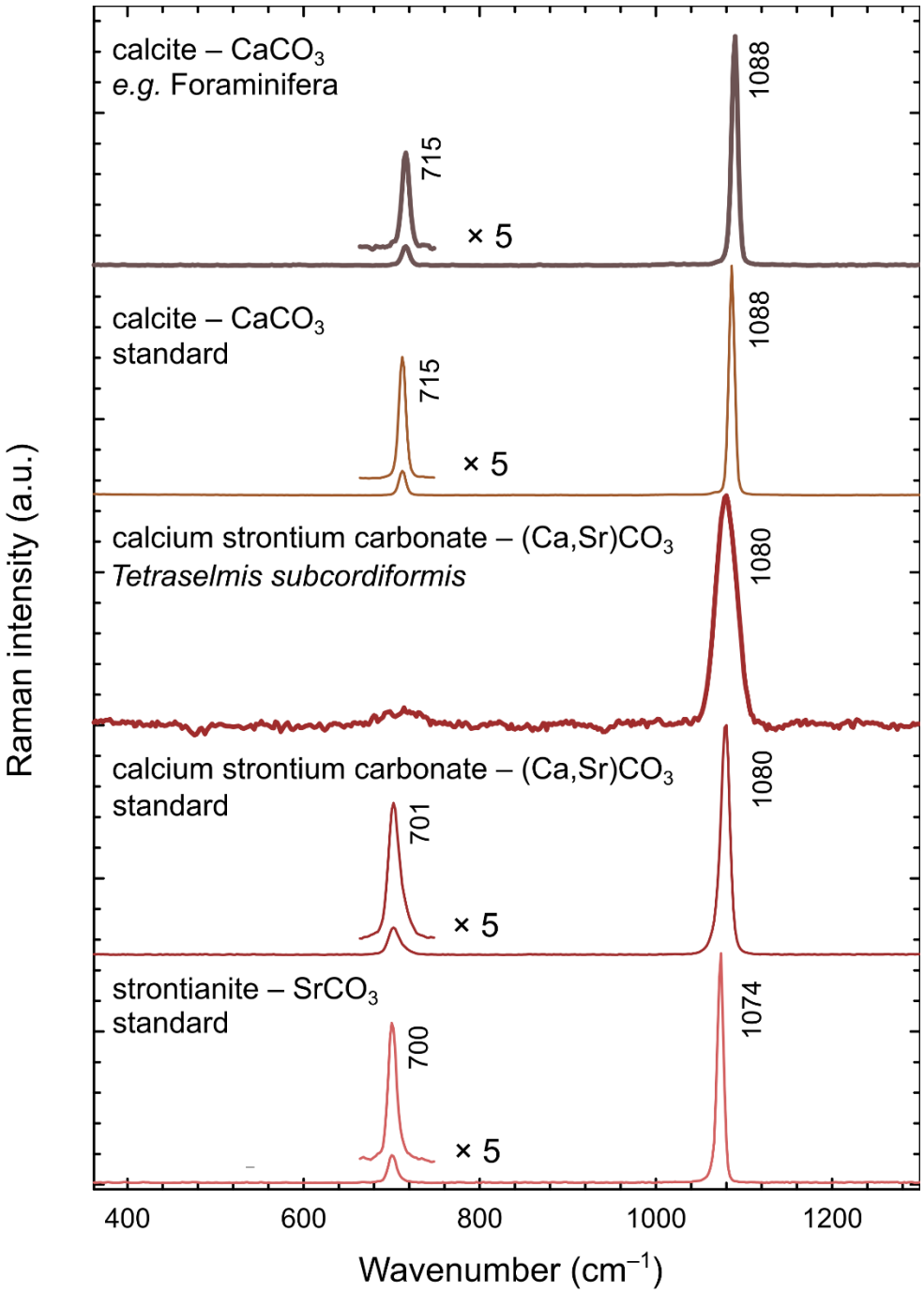

Fig. S3.

Representative Raman spectra of carbonate minerals observed in inspected species, all of them strongly polarize light: calcite or calcium carbonate ($CaCO_3$) found in various diatoms, Foraminifera, multicellular Rhodophytes and seaweed with respective standard and the mixture of calcium and strontium carbonates ($(Ca,Sr)CO_3$) found in *Tetraselmis* sp. with respective standards of pure chemical substances.

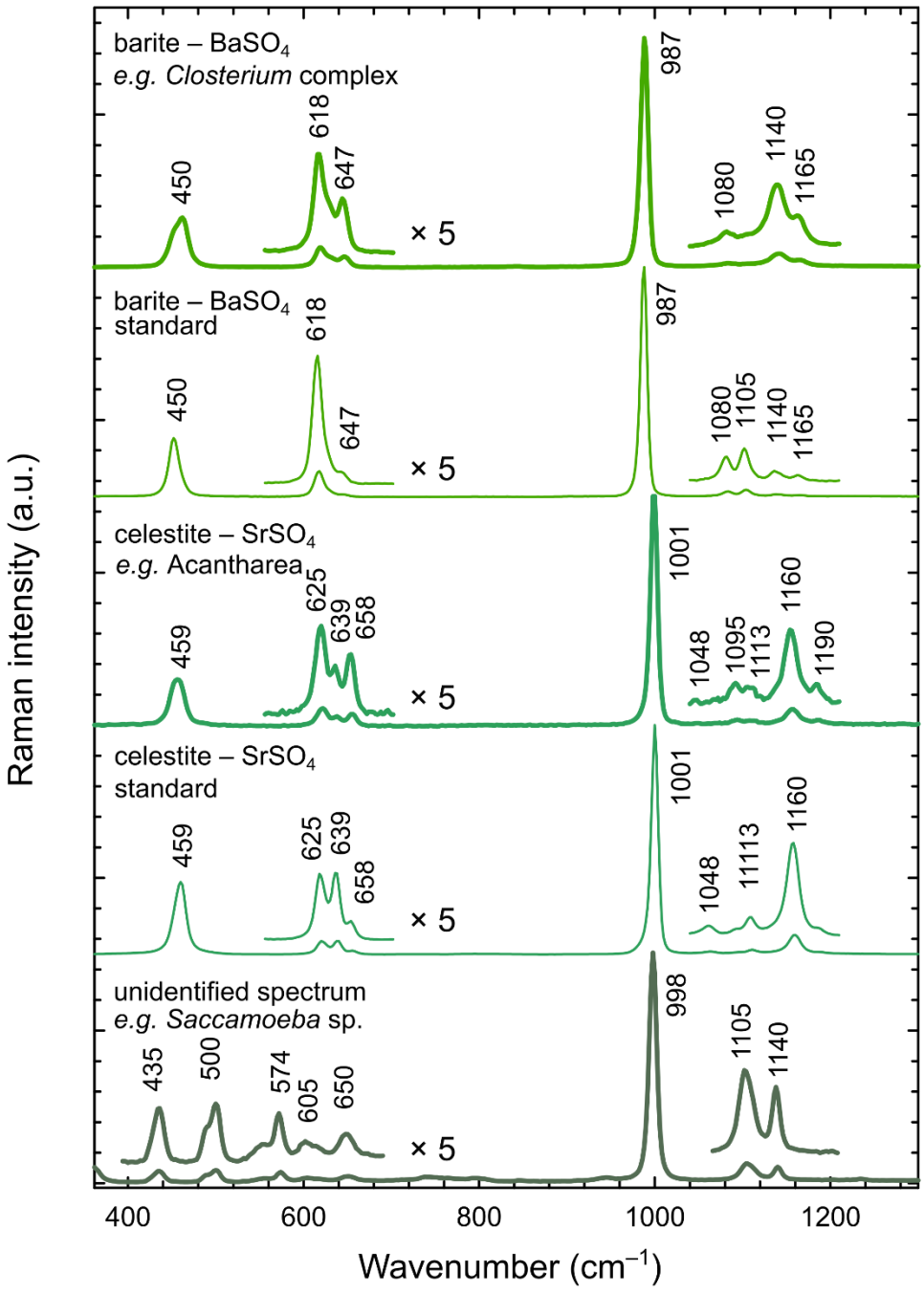

499

500 **Fig. S4.**

501 Representative Raman spectra of sulfate minerals observed in inspected species followed by
502 respective standards of pure chemical substances, all of them faintly polarize light: baryte ($BaSO_4$)
503 found in *Closterium peracerosum-strigosum-littorale* complex, *Cosmarium* sp., *Spirogyra* sp.,
504 celestite ($SrSO_4$) found in skeletons of Acantharea, and unidentified spectra of sulfate resembling
505 minerals mixed with lipophilic organic matter found in *Saccamoeba* sp. Raman spectra of sulfates
506 show variability in dependence of crystal orientation and minor admixtures of other salts.
507

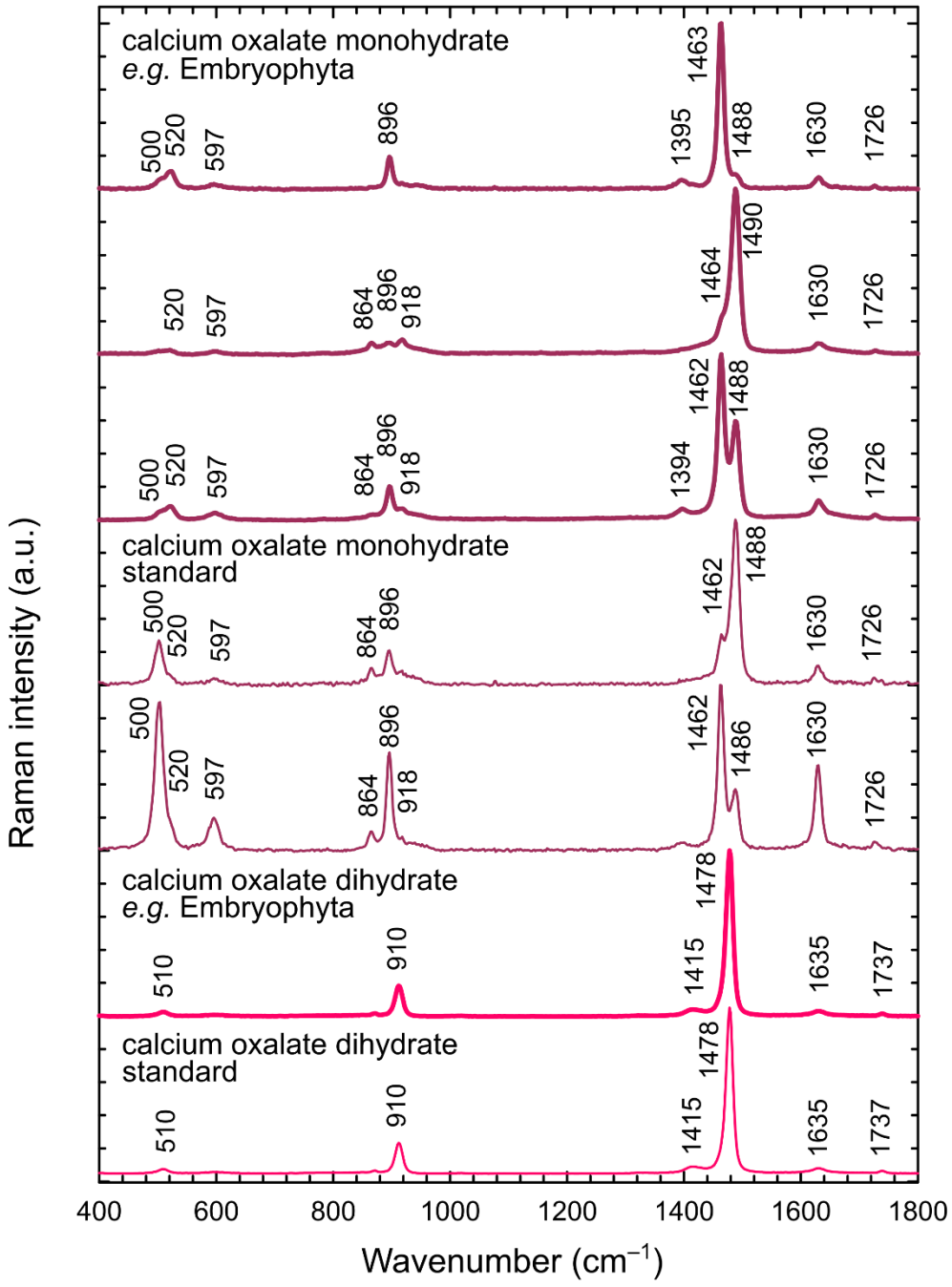

508

509 **Fig. S5.**

510 Representative Raman spectra of organic crystals polarizing light observed in inspected species
511 followed by respective standards of pure chemical substances. The crystals of calcium oxalate
512 monohydrate strongly polarize Raman signal – the major peaks interchange their relative
513 intensities according to the crystal orientation with respect of polarization plane of the excitation
514 beam. It was found in Coleochaetophyceae, Zygnematophyceae, Embryophyta. The calcium
515 oxalate dihydrate was found in Embryophyta.

516

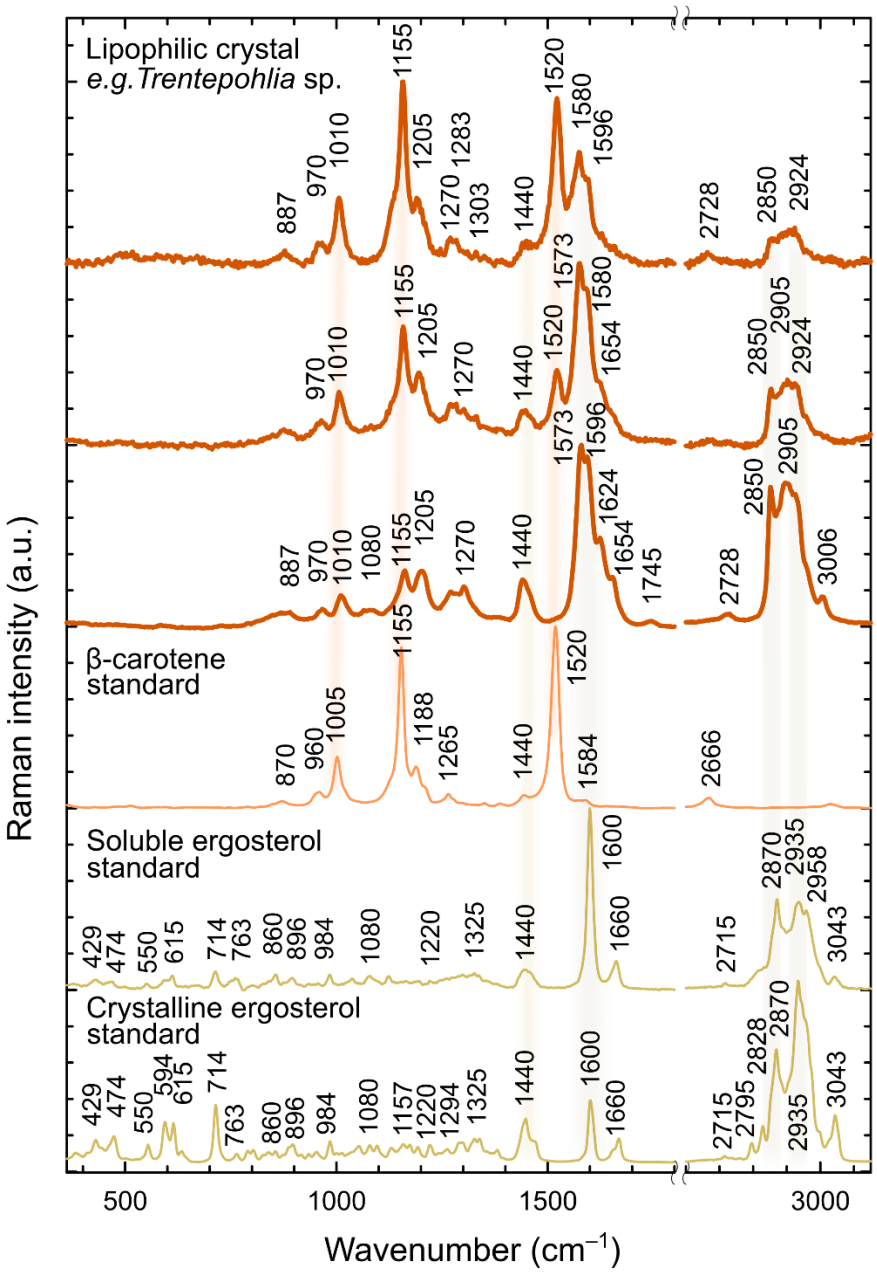

Fig. S6.

Representative Raman spectra of organic crystals polarizing light observed in inspected species followed by respective standards of pure chemical substances: lipophilic crystalline mixtures of carotenoids and sterols found in ulvophytes *Trentepohlia* sp. and *Scotinosphaera giberosa*, rhodophyte *Asterocytis ramonsa* and cyanobacteria *Oscillatoria* sp. Raman measurements using a high-intensity laser beam lead to photo-degradation of carotenoids present in the structure, thus their Raman signal decreases over time and allows observation of other admixtures in greater detail. We failed to find a precisely matching standard for sterols forming these lipophilic crystals; the biogenic crystals may contain a complex mixture of various chemical species.

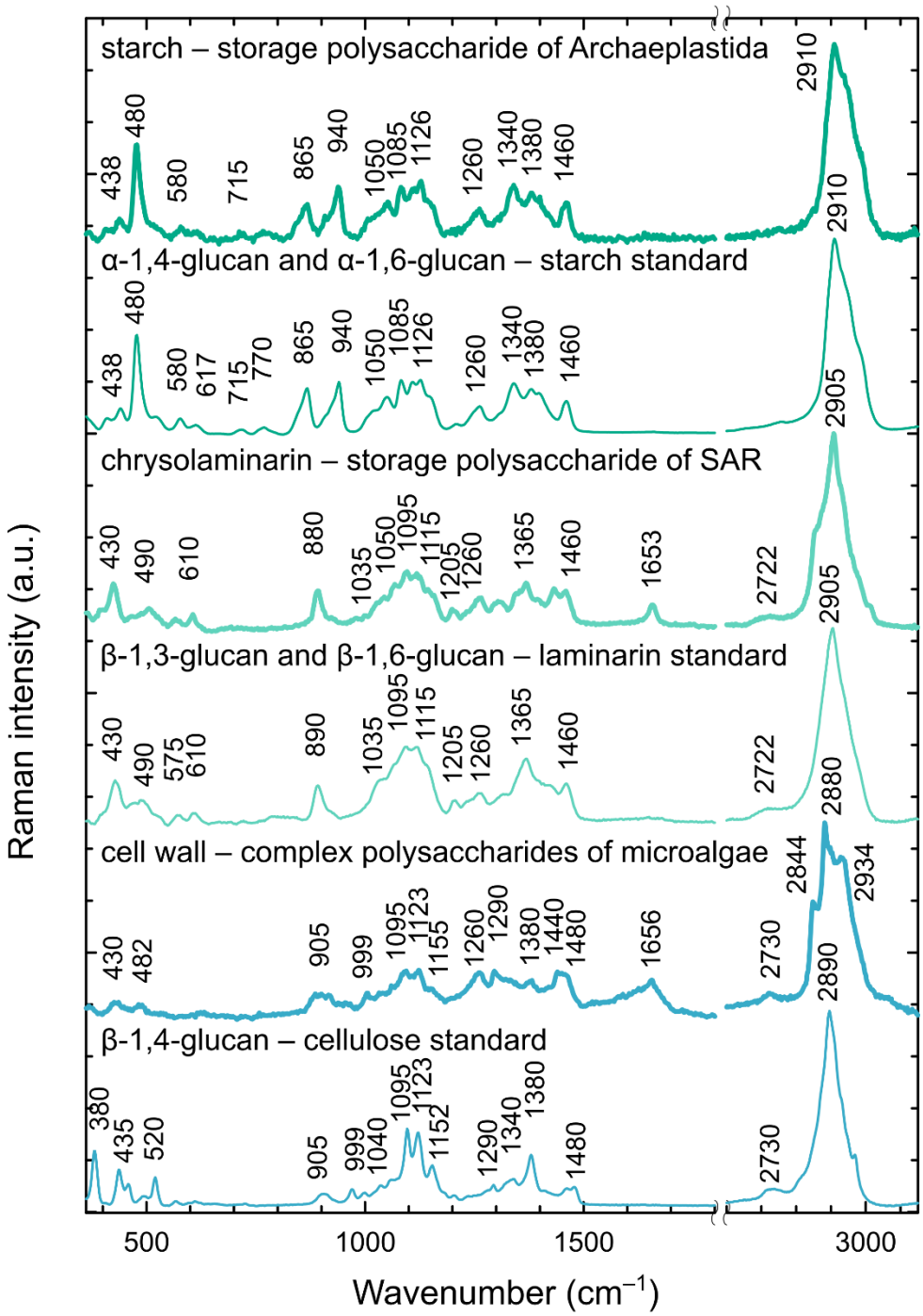

Fig. S7.

Representative Raman spectra of light polarizing polysaccharides in inspected species with respective standards of pure chemical substances: starch – storage polysaccharide of α-1,4-glucan and α-1,6-glucan found in Archaeplastida, chrysolaminarin – storage polysaccharide of β-1,3-glucan and β-1,6-glucan found in SAR, cellulose – structure polysaccharide of β-1,4-glucan forming cell walls of various microalgae (both Archaeplastida and SAR).

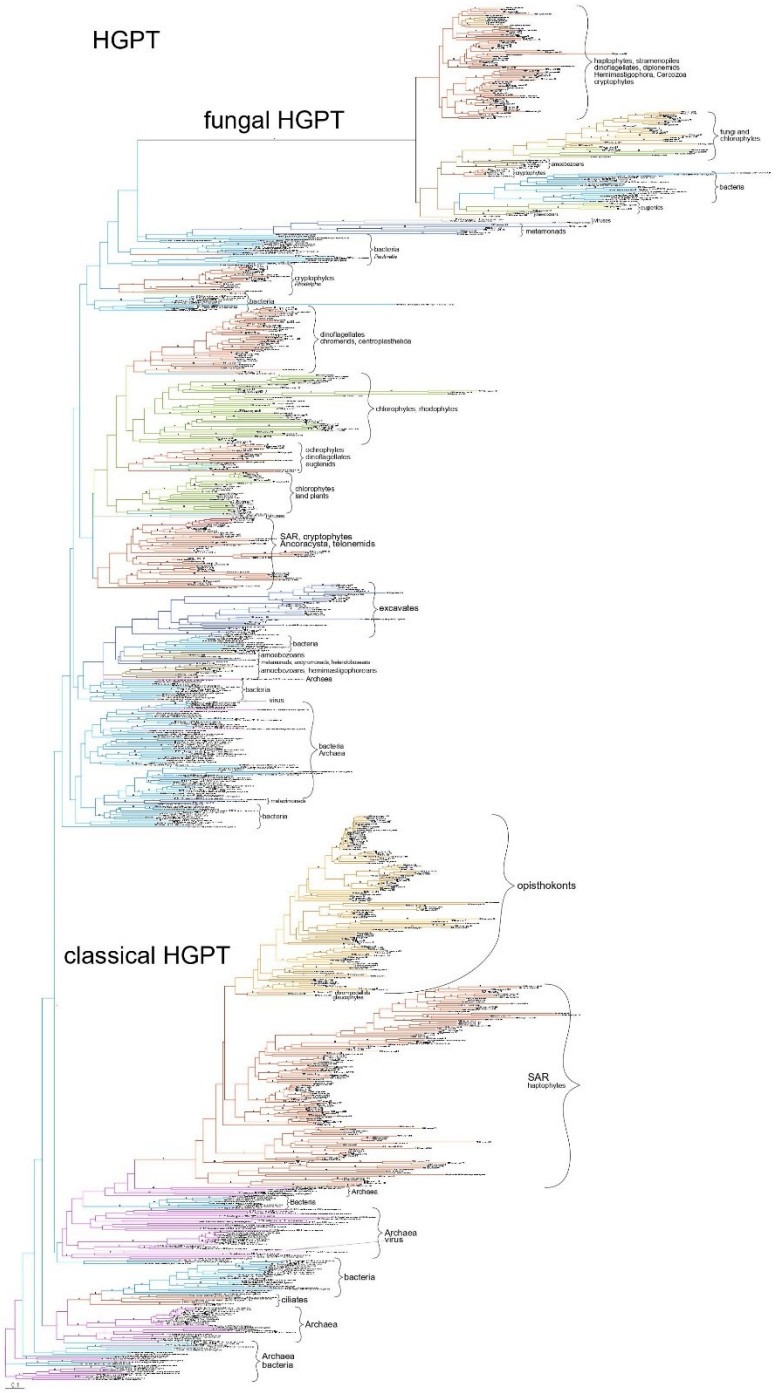

535

536 **Fig. S8.**

537 Maximum likelihood tree of hypoxanthine-guanine phosphoribosyl transferase (HGPT) as
538 inferred from amino acid sequences (171 aa). Numbers above branches indicate bootstrap
539 support (200 replicates).

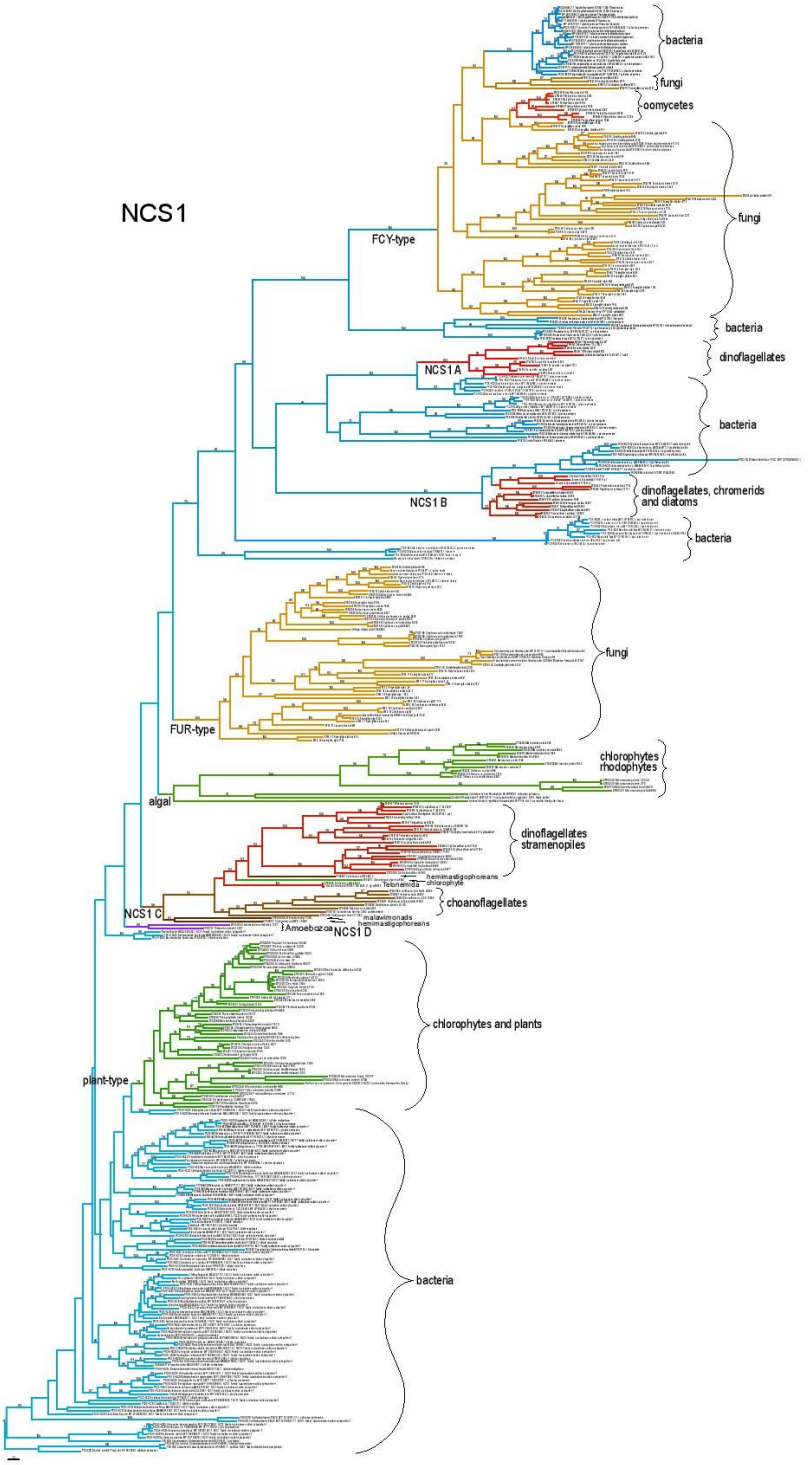

Fig. S9.

Maximum likelihood tree of nucleobase-cation symporter 1 (NCS1) as inferred from amino acid sequences (463 aa positions). Numbers above branches indicate bootstrap support (200 replicates).

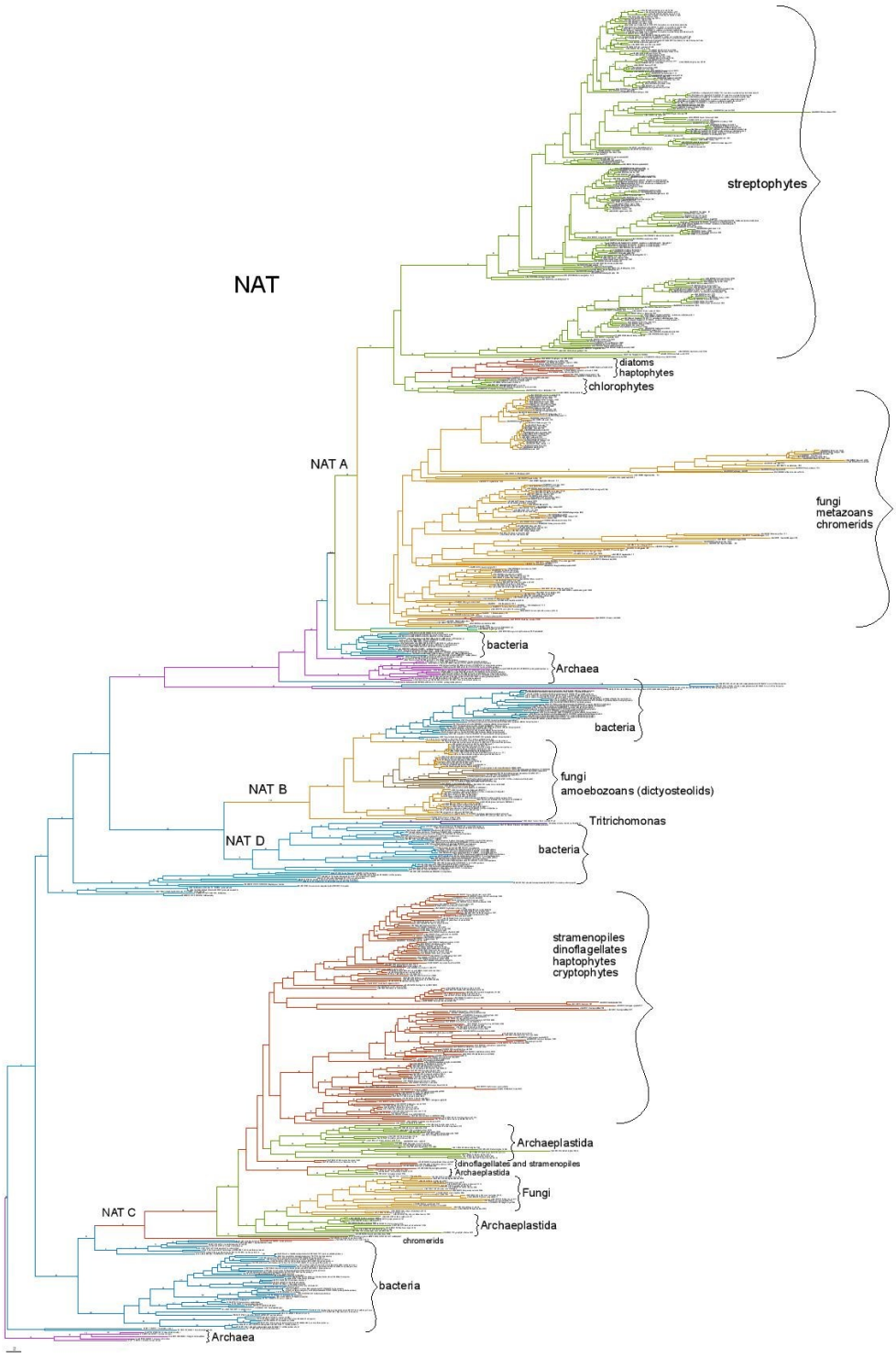

Fig. S10.

Maximum likelihood tree of nucleobase-ascorbate transporter (NAT) as inferred from amino acid sequences (385 aa). Numbers above branches indicate bootstrap support (200 replicates).

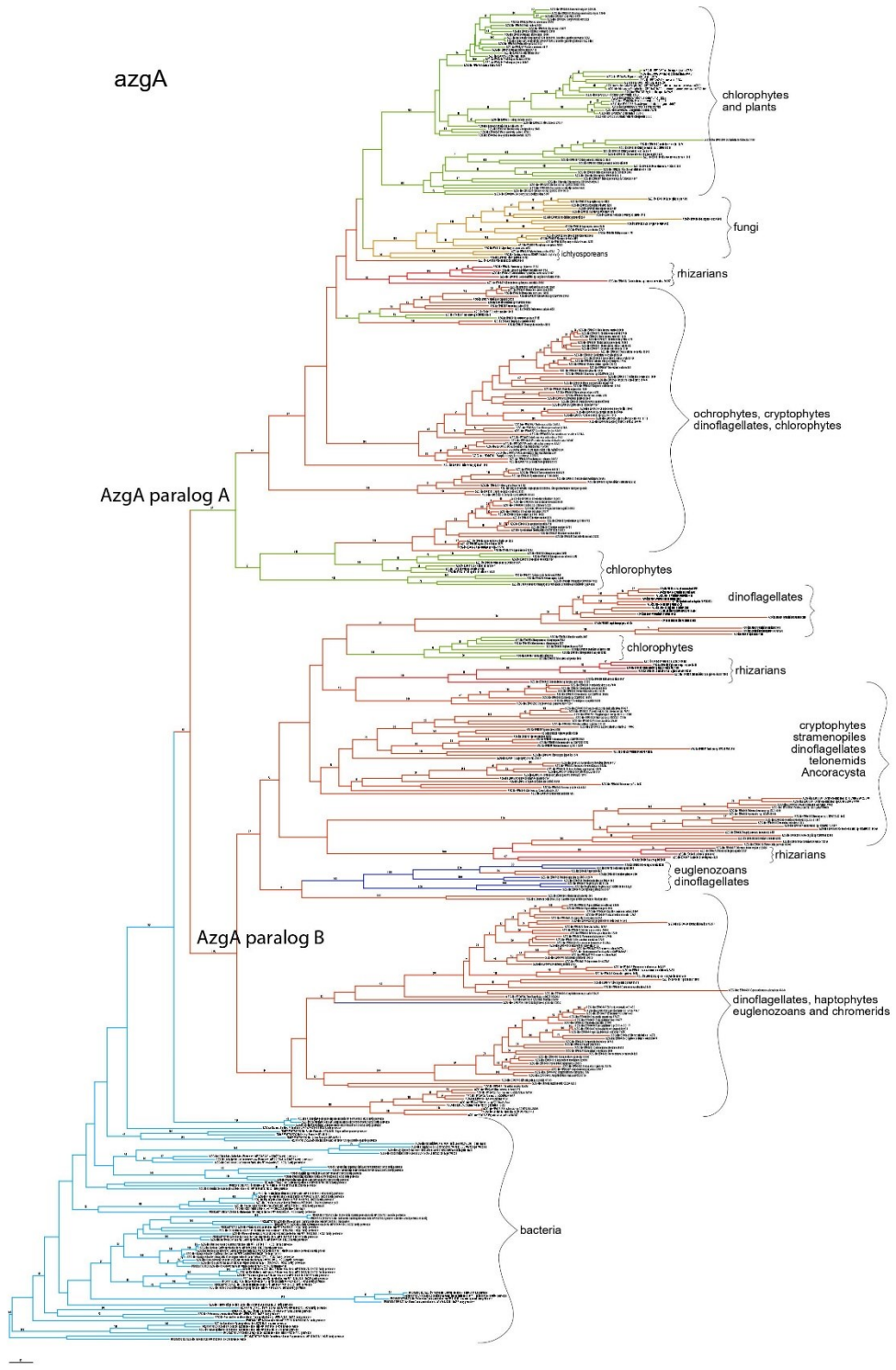

550

551 **Fig. S11.**

552 Maximum likelihood tree of AzgA as inferred from amino acid sequences (395 aa). Numbers
553 above branches indicate ML bootstrap support (200 replicates).

554

Table S1. Overview of the cell inclusions present in eukaryotes and cyanobacteria and their identification *via* Raman microscopy and light polarization. Species are listed according to their taxonomic classification and then alphabetically – species positively tested for purine inclusions (in black) and not positively tested for purine inclusions (in grey); capital letters in brackets refer to the phylogeny scheme in Fig. 1; (b) stands for biotechnologically important species and (m) for model organism. **Habitat – trophy:** E – endobiont, F – freshwater, Hp – halophilic, M – marine, S – snow, T – terrestrial; a – autotroph, h – heterotroph, p – parasite. **Culture collections:** ATCC – American Type Culture Collection, Manassas, USA; CAUP – Culture Collection of Algae of Charles University in Prague, Czech Republic; CCALA – Culture collection of Autotrophic Organisms of the Institute of Botany of the AS CR, Třeboň, Czech Republic; CCAP – Culture Collection of Algae and Protozoa, Orban, UK; CCF – Culture collection of Fungi, Praha, Czech Republic; CCMP – Culture Collection of Marine Phytoplankton – part of NCMA: NCMA – National Center for Marine Algae and Microbiota, Bigelow, USA; CRC – Chlamydomonas Resource Center, University of Minnesota, St. Paul, USA; CVCC – China Veterinary Culture Collection Center, National Control Institute of Veterinary Bio-products and Pharmaceutical (NCIVBP), Ministry of Agriculture, Beijing, China; DBM – Department of Biochemistry and Microbiology at University of Chemistry and Technology, Prague, Czech Republic; EUROSCARF – EUROpean Saccharomyces Cerevisiae Archive for Functional analysis, Scientific Research and Development GmbH, Oberursel, Germany; NIES – National Institute for Environmental Studies, Tsukuba, Japan; NCMA – CCMP - National Center for Marine Algae and Microbiota, Culture Collection of Marine Phytoplankton, Bigelow, USA; priv – private collection; RCC – Roscoff Culture Collection, Roscoff, France; SAG – Culture Collection of Algae at Goettingen University, Germany; UTEX – University of Texas at Austin, USA

Cultivation method:

– – no cultivation prior to observations and measurements (in case of environmental samples)
ASW-D – Artificial Sea Water for Diplonemids according to [46], 20 °C
ASW-L – Artificial Sea Water for Labyrinthulomycetes: 3,5% artificial sea water supplied with 1 g of yeast extract and 10 g of glucose, 25 °C
BBM – Basal Bold's Medium according to [47], 20–25 °C, 16:8 h light:dark cycle
BHI – Brain Heart Infusion medium as described in [48]
DY-IV – medium according to [49], 15 °C, 12:12 h light:dark cycle
f/2 – medium according to [50], 20–25 °C, 16:8 h light:dark cycle
f/2B – f/2 medium according to [50] with addition of sterile barley grain, 20–25 °C
Fw – ATCC 802 Sonneborn's Paramecium medium, 20–25 °C
FwAM – Fresh Water Amoeba Medium – ATCC medium 997, 20–25 °C
FwB1 – 25% ATCC 802 Sonneborn's Paramecium medium, with addition of sterile barley grain, 20–25 °C
FwB2 – 25% ATCC 802 Sonneborn's Paramecium medium, with addition of sterile barley grain, 17 °C
HM-V – Halophiles Medium number V according to [51] with addition of sterile barley grain, 20–25 °C
JM – ATCC 1525, 25 °C
LB – 3% Lysogeny Broth medium according to [52], 25 °C
LBM – 3% Lysogeny Broth medium according to [52] in Artificial Sea Water, 25 °C

M7 – medium according to[53], 25 °C
MAM – Marine Amoeba Medium – ATCC medium 994, 25 °C
MEA – Malt Extract Agar according to [54], 25 °C
MS-1 – Murashige and Skoog liquid medium according to [55], 25 °C, 16:8 h light:dark cycle
MS-2 – Murashige and Skoog solid medium according to [55], 25 °C, 16:8 h light:dark cycle
Neff – medium of Neff and Neff according to [56], 25 °C
OG – oat grain on cellulose paper kept in 100% humidity, 25 °C
PDA – Potato Dextrose Agar according to [57], 25 °C
PYGC – Proteose peptone – Yeast extract – Glucose–Cysteine medium according to [58], 25 °C
TYI – ATCC 2695 Keister's Modified TYI-S-33 medium, 37 °C
TYM – medium modified according to [59] by an overlay of inactivated horse serum, 25 °C
YPAD – ATCC 1069 medium, 37 °C
† – fixed cells
* – supplementary guanine added (approximately 30 µM final concentration), sterilized by 0.22µm filtration
[#] – same species has been measured previously for publication in [3]

Cult. coll.	Code	Species	Habitat -trophy	Taxonomic classification	Raman identity	Cult. method
priv		*Eimeria maxima* **(A)** (m)	E h p	SAR – Alveolata – **Apicomplexa –** Coccidia	Guanine	†
priv		*Psychodiella sergenti*	E h p	SAR – Alveolata – **Apicomplexa –** Gregarinasina	Guanine	–
NCMA	CCMP3155	*Vitrella brassicaformis*	M a	SAR – Alveolata – **Chrompodellids** – Vitrellaceae	Guanine	–
ns		*Coleps* sp.	F h	SAR – Alveolata – **Ciliophora –** Prostomatea	Starch	–
ns		*Cyclidium* sp.	F h	SAR – Alveolata – **Ciliophora –** Oligohymenophorea	Guanine	–
ns		*Euplotes* sp.	F h	SAR – Alveolata – **Ciliophora –** Spirotrichea	Guanine	–
ns		*Euplotes* sp.	M h	SAR – Alveolata – **Ciliophora –** Spirotrichea	Guanine	–
ns		*Halteria* sp.	F h	SAR – Alveolata – **Ciliophora –** Spirotrichea	Guanine	–
ns		*Glaucoma* sp.	F h	SAR – Alveolata – **Ciliophora –** Oligohymenophorea	Guanine	–
ns		Hypotrichia gen. sp.	M h	SAR – Alveolata – **Ciliophora –** Spirotrichea	Guanine	–
ns		*Lembadion* sp.	M h	SAR – Alveolata – **Ciliophora –** Oligohymenophorea	Guanine	–
ns		*Oxytricha* gen. sp.	F h	SAR – Alveolata – **Ciliophora –** Spirotrichea	Guanine	–
ns		*Paramecium* sp. **(C)** (m)	F h	SAR – Alveolata – **Ciliophora –** Oligohymenophorea	Guanine	†
ns		Scuticulociliatia gen. sp.	M h	SAR – Alveolata – **Ciliophora –** Oligohymenophorea	Guanine	–
ns		*Vorticella* sp.	F h	SAR – Alveolata – **Ciliophora –** Oligohymenophorea	–	–
priv		*Borghiella* sp.	F a	SAR – Alveolata – **Dinoflagellata** – Suessiales	Guanine	–
NCMA	CCMP449	*Heterocapsa triquetra*	M a	SAR – Alveolata – **Dinoflagellata** – Peridiniales	Guanine	f/2
priv		*Glenodinium foliaceum* **(B)**	M a	SAR – Alveolata – **Dinoflagellata** – Peridiniales	Guanine	–
ns		*Gymnodinium* sp.	F a	SAR – Alveolata – **Dinoflagellata** – Gymnodiniales	Guanine	–
ns		*Peridinium* sp.	F a	SAR – Alveolata – **Dinoflagellata** – Peridiniales	Guanine	–
priv		*Sphaerodinium* sp.	F a	SAR – Alveolata – **Dinoflagellata** – Suessiales	Guanine	–
priv	370	*Symbiodinium microadriaticum* (m)	M a	SAR – Alveolata – **Dinoflagellata** – Suessiales	Guanine	f/2
NCMA	CCMP829	*Symbiodinium tridacnidorum*	M a	SAR – Alveolata – **Dinoflagellata** – Suessiales	Guanine	f/2
ns		*Symbiodinium* sp. isolated from *Capnella imbricata*	M a	SAR – Alveolata – **Dinoflagellata** – Suessiales	Guanine	f/2
CAUP	J95	*Achnanthidium* sp.	F a	SAR – Stramenopiles – **Ochrophyta** – **Bacillariophyceae**	Calcite	–
ns		*Asterionella formosa*	F a	SAR – Stramenopiles – **Ochrophyta** – **Bacillariophyceae**	–	–
ns		*Aulacoseira* sp.	F a	SAR – Stramenopiles – **Ochrophyta** – **Bacillariophyceae**	–	–
ns		*Encyonema* sp.	F a	SAR – Stramenopiles – **Ochrophyta** – **Bacillariophyceae**	Uric acid	–
ns		*Entomoneis ornata*	M a	SAR – Stramenopiles – **Ochrophyta** – **Bacillariophyceae**	–	–
ns		*Fragilaria* sp.	F a	SAR – Stramenopiles – **Ochrophyta** – **Bacillariophyceae**	Uric acid	–
ns		*Frustulia* sp.	F a	SAR – Stramenopiles – **Ochrophyta** – **Bacillariophyceae**	–	–
ns		*Gomphonema truncatum*	F a	SAR – Stramenopiles – **Ochrophyta** – **Bacillariophyceae**	–	–

Cult. coll.	Code	Species	Habitat -trophy	Taxonomic classification	Raman identity	Cult. method
ns		*Licmophora* sp.	M a	SAR – Stramenopiles – **Ochrophyta** – **Bacillariophyceae**	Calcite	–
ns		*Melosira* sp.	F a	SAR – Stramenopiles – **Ochrophyta** – **Bacillariophyceae**	–	–
ns		*Navicula cryptocephala*	F a	SAR – Stramenopiles – **Ochrophyta** – **Bacillariophyceae**	Uric acid	–
ns		*Navicula* sp.	F a	SAR – Stramenopiles – **Ochrophyta** – **Bacillariophyceae**	Uric acid Xanthine	–
ns		Naviculaceae gen. sp., *Seminavis*-like	M a	SAR – Stramenopiles – **Ochrophyta** – **Bacillariophyceae**	Guanine	–
ns		*Paralia sulcata*	M a	SAR – Stramenopiles – **Ochrophyta** – **Bacillariophyceae**	Calcite	–
CCAP	1052/1B	*Phaeodactylum tricornutum* (m)	M a	SAR – Stramenopiles – **Ochrophyta** – **Bacillariophyceae**	Calcite	f/2
ns		*Pinnularia viridis*	F a	SAR – Stramenopiles – **Ochrophyta** – **Bacillariophyceae**	–	–
ns		*Pleurosigma* sp.	M a	SAR – Stramenopiles – **Ochrophyta** – **Bacillariophyceae**	Uric acid	–
ns		*Stauroneis phoenicenteron*	F a	SAR – Stramenopiles – **Ochrophyta** – **Bacillariophyceae**	–	–
NCMA	CCMP1335	*Thalassiosira pseudonana* (m)	M a	SAR – Stramenopiles – **Ochrophyta** – **Bacillariophyceae**	–	f/2
ns		*Spumella* sp.	F a	SAR – Stramenopiles – **Ochrophyta** – **Synurophyceae**	Guanine	–
CAUP	B710	*Synura hibernica*	F a	SAR – Stramenopiles – **Ochrophyta** – **Synurophyceae**	Guanine	–
CAUP	H4302	*Eustigmatos polyphem* (b)	T a	SAR – Stramenopiles – **Ochrophyta** – **Eustigmatophyceae**	Guanine	BBM
NIES	2146	*Nannochloropsis oculata* **(K)** (b) (m)	M a	SAR – Stramenopiles – **Ochrophyta** – **Eustigmatophyceae**	Guanine	f/2
NIES	2860	*Vacuoliviride crystalliferum*[#]	Un a	SAR – Stramenopiles – **Ochrophyta** – **Eustigmatophyceae**	Guanine Chrysolaminarin	BBM
ns		*Cystoseira* sp.	M a	SAR – Stramenopiles – **Ochrophyta** – **Phaeophyceae**	Calcite	–
ns		*Dictyota dichotoma*	M a	SAR – Stramenopiles – **Ochrophyta** – **Phaeophyceae**	Calcite	–
ns		*Padina pavonica*	M a	SAR – Stramenopiles – **Ochrophyta** – **Phaeophyceae**	Calcite	–
ns		*Actinophrys* sp.	F a	SAR – Stramenopiles – **Ochrophyta** – **Actinophryidae**	Guanine	–
ns		*Gonyostomum* sp.	F a	SAR – Stramenopiles – **Ochrophyta** – **Raphidophyceae**	Guanine	–
CAUP	D301	*Botrydiopsis intercedens*	F a	SAR – Stramenopiles – **Ochrophyta** – **Xanthophyceae**	Guanine	BBM
UTEX	B 2999	*Heterococcus* sp.	F a	SAR – Stramenopiles – **Ochrophyta** – **Xanthophyceae**	–	BBM
ns		*Ophiocytium* sp.	F a	SAR – Stramenopiles – **Ochrophyta** – **Xanthophyceae**	Guanine	–
CCALA	517	*Tribonema aequale* **(F)** (m)	F a	SAR – Stramenopiles – **Ochrophyta** – **Xanthophyceae**	Guanine	BBM
ns		*Xanthonema* sp.	F a	SAR – Stramenopiles – **Ochrophyta** – **Xanthophyceae**	Guanine	–
DBM	CO3I	*Schizochytrium* sp. (b) (m)	M h	SAR – Stramenopiles – **Labyrinthulomycota**	Guanine	ASW-L
priv		*Cafeteria roenbergensis*	M h	SAR – Stramenopiles – **Bicosoecida**	–	f/2*
priv		*Cafileria marina*	M h	SAR – Stramenopiles – **Bicosoecida**	Guanine	f/2*
CCF	3762	*Phytophthora cactorum*	E h	SAR – Stramenopiles – **Oomycota**	–	PDA

Cult. coll.	Code	Species	Habitat -trophy	Taxonomic classification	Raman identity	Cult. method
CCF	4738	*Phytophthora rosacearum*-like	E h	SAR – Stramenopiles – **Oomycota**	–	PDA
priv	Ther	*Blastocystis* sp. isolated from *Testudo hermanni*	E h	SAR – Stramenopiles – **Opalinata –** Blastocystae	–	TYM
NCMA	CCMP2755	*Bigelowiella natans* **(L)** (m)	M a	SAR – Rhizaria – **Cercozoa** – **Chlorarachnea**	Guanine	f/2
priv	LITO	Cercomonadida gen. sp.	F h	SAR – Rhizaria – **Cercozoa** – **Cercomonadida**	Guanine	Fw
ns		*Viridiraptor invadens*	F h	SAR – Rhizaria – **Cercozoa** – **Viridiraptoridae**	Guanine	–
ns		*Euglypha* sp.	F h	SAR – Rhizaria – **Cercozoa – Euglyphida**	Guanine	–
ns		*Trinema* sp.	F h	SAR – Rhizaria – **Cercozoa – Euglyphida**	Guanine	–
ns		*Marinomyxa marina*	M h	SAR – Rhizaria – Endomyxa **– Phytomyxea**	–	–
ns		Acantharea gen. sp.	M h	SAR – Rhizaria – **Retaria** – Acantharea	Celestite	†
ns		Globigerinidae gen. sp.	M h	SAR – Rhizaria – **Retaria** – Foramanifera	–	†
ns		Globorotaliidae gen. sp.	M h	SAR – Rhizaria – **Retaria** – Foramanifera	Calcite	†
priv	LIS-Tel	*Telonema* sp.	M h	**Telonemida**	Guanine	f/2B*
NCMA	CCMP371	*Emiliania huxleyi* (m)	M a	Haptista – **Haptophyta**	Guanine	f/2*
RCC	RCC1350	*Isochrysis* sp. **(M)** (b)	M a	Haptista – **Haptophyta**	Xanthine Uric acid	f/2*
ns		*Raphidiophrys* sp.	F h	Haptista – **Centroplasthelida**	Guanine	–
CAUP	F105	*Cryptomonas* sp. (O)	F a	Cryptista – **Cryptophyta**	Uric acid	BBM
ns		*Chroomonas* sp.	F a	Cryptista – **Cryptophyta**	Uric acid Guanine monohydrate	–
CAUP	O101	*Glaucocystis nostochinearum*	F a	Archaeplastida – **Glaucophyta**	Xanthine	BBM
ns		*Asparagopsis taxiformis*	M a	Archaeplastida – **Rhodophyta – Florideophyceae**	Calcite	–
CAUP	L201	*Asterocytis ramosa*	M a	Archaeplastida – **Rhodophyta – Bangiophyceae**	Carotenoids, lipids	f/2
CCALA	971	*Audouinella* sp.	M a	Archaeplastida – **Rhodophyta – Florideophyceae**	–	f/2
ns		*Ceramium* sp.	M a	Archaeplastida – **Rhodophyta – Florideophyceae**	Calcite	–
ns		*Hildebrandia rivularis*	M a	Archaeplastida – **Rhodophyta – Florideophyceae**	–	–
CCALA	416	*Porphyridium purpureum* (b)	M a	Archaeplastida – **Rhodophyta – Porphyridiophyceae**	–	f/2
CCALA	925	*Rhodella violacea*	M a	Archaeplastida – **Rhodophyta – Rhodellophyceae**	Lipids	f/2
ns		*Asterococcus* sp.	F a	Archaeplastida – Viridiplantae – Chlorophyta – **Chlorophyceae**	Guanine	–
ns		*Bulbochaete* sp.	F a	Archaeplastida – Viridiplantae – Chlorophyta – **Chlorophyceae**	Guanine	–
CRC	CC-1690	*Chlamydomonas reinhardtii*[#] (m)	F a	Archaeplastida – Viridiplantae – Chlorophyta – **Chlorophyceae**	Guanine	BBM
CAUP	G224	*Chlamydomonas geitleri*	F a	Archaeplastida – Viridiplantae – Chlorophyta – **Chlorophyceae**	Guanine	BBM

Cult. coll.	Code	Species	Habitat -trophy	Taxonomic classification	Raman identity	Cult. method
ns		*Chlamydomonas* sp.	F a	Archaeplastida – Viridiplantae – Chlorophyta – **Chlorophyceae**	Guanine	–
priv	AMAZONIE	*Chlamydomonadales* gen. sp.	F h	Archaeplastida – Viridiplantae – Chlorophyta – **Chlorophyceae**	Guanine	Fw
priv	KBEL1C	*Polytoma* sp.	F h	Archaeplastida – Viridiplantae – Chlorophyta – **Chlorophyceae**	Guanine	Fw
CAUP	H 6902	*Chlorochytrium lemnae*	E – F a	Archaeplastida – Viridiplantae – Chlorophyta – **Chlorophyceae**	Guanine	BBM
priv		*Chloromonas arctica*	S a	Archaeplastida – Viridiplantae – Chlorophyta – **Chlorophyceae**	Guanine	BBM
ns		*Desmodesmus quadricauda* (m)	F a	Archaeplastida – Viridiplantae – Chlorophyta – **Chlorophyceae**	Guanine	–
ns		*Desmodesmus* sp.	F a	Archaeplastida – Viridiplantae – Chlorophyta – **Chlorophyceae**	Guanine	–
ns		*Eudorina* sp.	F a	Archaeplastida – Viridiplantae – Chlorophyta – **Chlorophyceae**	Guanine	–
ns		*Gleocystis* sp.	F a	Archaeplastida – Viridiplantae – Chlorophyta – **Chlorophyceae**	Guanine	–
ns		*Microspora* sp.	F a	Archaeplastida – Viridiplantae – Chlorophyta – **Chlorophyceae**	Guanine	–
ns		*Monactinus simplex*	F a	Archaeplastida – Viridiplantae – Chlorophyta – **Chlorophyceae**	Guanine	–
CAUP	H2908	*Monoraphidium contortum* (b)	F a	Archaeplastida – Viridiplantae – Chlorophyta – **Chlorophyceae**	Guanine	BBM
ns		*Oedogonium* sp.	F a	Archaeplastida – Viridiplantae – Chlorophyta – **Chlorophyceae**	Guanine	–
ns		*Pediastrum boryanum*	F a	Archaeplastida – Viridiplantae – Chlorophyta – **Chlorophyceae**	Guanine	–
CAUP	H2308	*Pediastrum duplex* **(I)**	F a	Archaeplastida – Viridiplantae – Chlorophyta – **Chlorophyceae**	Guanine	BBM
ns		*Tetraedron* sp.	F a	Archaeplastida – Viridiplantae – Chlorophyta – **Chlorophyceae**	Guanine	–
ns		*Tetraspora* sp.	F a	Archaeplastida – Viridiplantae – Chlorophyta – **Chlorophyceae**	Guanine	–
CAUP	H 1917	*Chlorella vulgaris* **(N)** (b) (m)	F a	Archaeplastida – Viridiplantae – Chlorophyta – **Trebouxiophyceae**	Xanthine	BBM*
CAUP	H 5107	*Coccomyxa elongata*	T a	Archaeplastida – Viridiplantae – Chlorophyta – **Trebouxiophyceae**	Guanine	BBM
ns		*Dictyosphaerium* sp. (b)	F a	Archaeplastida – Viridiplantae – Chlorophyta – **Trebouxiophyceae**	Uric acid	–
ns		*Keratococcus* sp.	F a	Archaeplastida – Viridiplantae – Chlorophyta – **Trebouxiophyceae**	Guanine	–
ns		*Micractinium* sp.	F a	Archaeplastida – Viridiplantae – Chlorophyta – **Trebouxiophyceae**	Guanine	–
CAUP	H8801	*Phyllosiphon arisari*	F a p	Archaeplastida – Viridiplantae – Chlorophyta – **Trebouxiophyceae**	Lipids	BBM
CAUP	H8605	*Symbiochloris tschermakiae*	E/T a	Archaeplastida – Viridiplantae – Chlorophyta – **Trebouxiophyceae**	Lipids	BBM
ns		*Anadyomene* sp.	M a	Archaeplastida – Viridiplantae – Chlorophyta – **Ulvophyceae**	Calcite	–
ns		*Cladophora* sp.	F a	Archaeplastida – Viridiplantae – Chlorophyta – **Ulvophyceae**	Guanine	–
ns		*Cladophora* sp.	M a	Archaeplastida – Viridiplantae – Chlorophyta – **Ulvophyceae**	Calcite	–
ns		*Enteromorpha* sp.	M a	Archaeplastida – Viridiplantae – Chlorophyta – **Ulvophyceae**	Calcite	–
CAUP	H5301	*Scotinosphaera gibberosa*	F/T a	Archaeplastida – Viridiplantae – Chlorophyta – **Ulvophyceae**	Carotenoids, lipids	BBM
CAUP	J1601	*Trentepohlia* sp.	T a	Archaeplastida – Viridiplantae – Chlorophyta – **Ulvophyceae**	Carotenoids, lipids	BBM

Cult. coll.	Code	Species	Habitat -trophy	Taxonomic classification	Raman identity	Cult. method
CAUP	M101	*Prasinocladus ascus*	M a	Archaeplastida – Viridiplantae – Chlorophyta – **Chlorodendrophyceae**	Guanine monohydrate Uric acid	–
CAUP	M201	*Tetraselmis subcordiformis* **(H)** (b)	M a	Archaeplastida – Viridiplantae – Chlorophyta – **Chlorodendrophyceae**	Guanine monohydrate Uric acid	f/2
RCC	RCC745	*Ostreococcus tauri* (m)	M a	Archaeplastida – Viridiplantae – Chlorophyta – **Mamiellophyceae**	–	f/2
ns		*Nephroselmis* sp.	M a	Archaeplastida – Viridiplantae – Chlorophyta – **Nephrophyceae**	Guanine	–
ns		*Pyramimonas* sp.	M a	Archaeplastida – Viridiplantae – Chlorophyta – **Pyramimonadophyceae**	Guanine	–
NIES	995	*Mesostigma viride*	F a	Archaeplastida – Viridiplantae – Streptophyta – **Mesostigmatophyta**	–	–
CAUP	H7601	*Chlorokybus atmophyticus*	T a	Archaeplastida – Viridiplantae – Streptophyta – **Chlorokybophyceae**	Guanine	BBM
NIES	2285	*Klebsormidium flaccidum*[#] **(P)**	T a	Archaeplastida – Viridiplantae – Streptophyta – **Klebsormidiophyceae**	Uric acid	BBM
ns		*Coleochaete* sp.	F a	Archaeplastida – Viridiplantae – Streptophyta – **Coleochaetophyceae**	Calcium oxalate	–
NIES	1604	*Chara braunii*	F a	Archaeplastida – Viridiplantae – Streptophyta – **Charophyceae**	–	–
CAUP	K 801	*Actinotaenium* sp.	F a	Archaeplastida – Viridiplantae – Streptophyta – **Zygnematophyceae**	Uric acid	BBM
NIES	67	*Closterium peracerosum-strigosum-littorale* complex (m)	F a	Archaeplastida – Viridiplantae – Streptophyta – **Zygnematophyceae**	Baryte Starch	BBM
ns		*Cosmarium* sp.	F a	Archaeplastida – Viridiplantae – Streptophyta – **Zygnematophyceae**	Uric acid Baryte	–
ns		*Cylindrocystis* sp.	T a	Archaeplastida – Viridiplantae – Streptophyta – **Zygnematophyceae**	Calcium oxalate	–
ns		*Euastrum humerosum*	F a	Archaeplastida – Viridiplantae – Streptophyta – **Zygnematophyceae**	Uric acid	–
CAUP	K101	*Mesotaenium caldariorum*	F a	Archaeplastida – Viridiplantae – Streptophyta – **Zygnematophyceae**	Uric acid Guanine monohydrate	BBM*
ns		*Mougeotia* sp.	F a	Archaeplastida – Viridiplantae – Streptophyta – **Zygnematophyceae**	Uric acid	–
ns		*Netrium* sp.	F a	Archaeplastida – Viridiplantae – Streptophyta – **Zygnematophyceae**	Uric acid	–
NIES	303	*Penium margaritaceum* **(Q)**	F a	Archaeplastida – Viridiplantae – Streptophyta – **Zygnematophyceae**	Uric acid	BBM
ns		*Spirogyra* sp.	F a	Archaeplastida – Viridiplantae – Streptophyta – **Zygnematophyceae**	Baryte	–
ns		*Staurastrum* sp.	F a	Archaeplastida – Viridiplantae – Streptophyta – **Zygnematophyceae**	Uric acid	–
ns		*Tetmemorus* sp.	F a	Archaeplastida – Viridiplantae – Streptophyta – **Zygnematophyceae**	Uric acid	–
ns		*Xanthidium* sp.	F a	Archaeplastida – Viridiplantae – Streptophyta – **Zygnematophyceae**	Uric acid	–
ns		*Halophila stipulacea*	M a	Archaeplastida – Viridiplantae – Streptophyta – **Embryophyta**	Calcium oxalate monohydrate, dihydrate	–

Cult. coll.	Code	Species	Habitat -trophy	Taxonomic classification	Raman identity	Cult. method
priv	BY-2	*Nicotiana tabacum*	T a	Archaeplastida – Viridiplantae – Streptophyta – **Embryophyta**	Calcium oxalate monohydrate	MS-1
priv		*Physcomitrela patens*	T a	Archaeplastida – Viridiplantae – Streptophyta – **Embryophyta**	Calcium oxalate monohydrate	MS-2
priv	BW2	*Hemimastix kukwesjijk*	F h	**Hemimastigophora**	Guanine	FwB2*
ns		*Entosiphon* sp.	F a	Excavata – Discoba – **Euglenozoa – Euglenida**	Guanine	–
ns		*Euglena* sp. (m)	F a	Excavata – Discoba – **Euglenozoa – Euglenida**	Guanine	–
NCMA	CCMP1594	*Eutreptiela gymnastica* **(D)** (m)	M a	Excavata – Discoba – **Euglenozoa – Euglenida**	Guanine	f/2
ns		*Lepocynclis oxyuris*	F a	Excavata – Discoba – **Euglenozoa – Euglenida**	Guanine	–
ns		*Monomorphina pyrum*	F a	Excavata – Discoba – **Euglenozoa – Euglenida**	Guanine	–
ns		*Phacus* sp.	F a	Excavata – Discoba – **Euglenozoa – Euglenida**	Guanine	–
priv	SVATBA	*Rhabdomonas* sp.	F h	Excavata – Discoba – **Euglenozoa – Euglenida**	Guanine	Fw
ns		*Trachelomonas* sp.	F a	Excavata – Discoba – **Euglenozoa – Euglenida**	Guanine	–
priv	RIOZ	Free-living Kinetoplastea gen. sp.	F h	Excavata – Discoba – **Euglenozoa – Kinetoplastea**	Guanine	Fw
ns		*Bodo* sp.	F h	Excavata – Discoba – **Euglenozoa – Kinetoplastea**	Guanine	–
priv	M09	*'jaculum'* gen. sp.	E h p	Excavata – Discoba – **Euglenozoa – Kinetoplastea**	–	BHI
priv		*Trypanosoma mega*	E h p	Excavata – Discoba – **Euglenozoa – Kinetoplastea**	–	BHI
priv	YPF 1621	*Namystynia karyoxenos*	M h	Excavata – Discoba – **Euglenozoa – Diplonemea**	Guanine	ASW-D
priv	1.7 clone	*Rhynchopus* sp.	M h	Excavata – Discoba – **Euglenozoa – Diplonemea**	Guanine	ASW-D
priv	DT1610	*Flectonema* sp.	M h	Excavata – Discoba – **Euglenozoa – Diplonemea**	Guanine monohydrate	ASW-D
priv	RUM4AN	*Psalteriomonas lanterna*	F h	Excavata – Discoba – **Heterolobosea**	Guanine	Fw
priv	NEG-M	*Naegleria gruberi* **(E)** (m)	F h	Excavata – Discoba – **Heterolobosea**	Guanine	M7*
priv	BUSSPRAND	*Velundella trypanoides*	M h	Excavata – Discoba – **Jakobida**	–	JM
priv	AND	*Stygiella agilis*	M h	Excavata – Discoba – **Jakobida**	–	JM
priv	SPINDL2	*Gyromonas ambulans*	F h	Excavata – **Metamonada** – Fornicata	Guanine	Fw*
priv	TUN2	*Hexamita* sp.	F h	Excavata – **Metamonada** – Fornicata	Guanine	Fw*
priv	LITO	*Trepomonas rotans*	F h	Excavata – **Metamonada** – Fornicata	Guanine	Fw*
priv	BREZ2C	*Trepomonas* sp.	F h	Excavata – **Metamonada** – Fornicata	Guanine	Fw*
priv	CONGO	*Trepomonas steinii*	F h	Excavata – **Metamonada** – Fornicata	Guanine	LB
priv	Ncub	*Macrotrichomonoides* sp. isolated from *Neotermes cubanus*	E h	Excavata – **Metamonada** – Parabasalia	Guanine	–
priv	249	*Gefionella okellyi* **(J)**	F h	**Malawimonadida**	Guanine	f/2B*
ATCC	HM-1:IMSS	*Entamoeba histolytica*	E h	Amoebozoa – Evosea – **Archamoebae**	Lipids	TYI*

Cult. coll.	Code	Species	Habitat -trophy	Taxonomic classification	Raman identity	Cult. method
ATCC	30984	*Mastigamoeba balamuthi*	F h	Amoebozoa – Evosea – **Archamoebae**	Xanthine Lipids	PYGC*
priv	GO7	*Mastigella eilhardi*	F h	Amoebozoa – Evosea – **Archamoebae**	Guanine	Fw*
ns		*Fuligo septica*	T h	Amoebozoa – Evosea – **Eumycetozoa**	Guanine	–
priv		*Physarum polycephalum*	T h	Amoebozoa – Evosea – **Eumycetozoa**	Xanthine	OG *
priv	Neff	*Acanthamoeba castellanii*	F h	Amoebozoa – **Discosea** – Centramoebia	Xanthine Lipids	Neff*
ns		*Mayorella* sp.	F h	Amoebozoa – **Discosea** – Flabellinia	Xanthine	–
ns		*Mayorella* sp.	M h	Amoebozoa – **Discosea** – Flabellinia	Xanthine	–
priv	WFP252	*Neoparamoeba* sp.	M h	Amoebozoa – **Discosea** – Flabellinia	–	MAM
ns		*Thecamoeba* sp.	F h	Amoebozoa – **Discosea** – Flabellinia	Guanine	–
ns		*Vannella* sp.	F h	Amoebozoa – **Discosea** – Flabellinia	Guanine	–
ns		*Difflugia* sp.	F h	Amoebozoa – **Tubulinea** – Arcellinida	Guanine	–
ns		*Rhizamoeba* sp.	F h	Amoebozoa – **Tubulinea** – Leptomyxida	–	–
ns		*Saccamoeba* sp.	F h	Amoebozoa – **Tubulinea** – Hartmannellidae	Unidentified	–
priv	MSEDG	*Saccamoeba* sp.	F h	Amoebozoa – **Tubulinea** – Hartmannellidae	Unidentified	FwAM*
priv	4391/I	*Vermamoeba vermiformis*	F h	Amoebozoa – **Tubulinea** – Echinamoebida	–	FwAM*
priv	LIS-Man	*Mantamonas* sp.	M h	CRuMs – **Mantamonadida**	–	f/2B*
priv	FB10	*Subulatomonas* sp.	M h	Obazoa – **Breviatea**	–	LBM
priv	C3C	Choanoflagellata gen. sp.	Hp h	Obazoa – Opisthokonta – **Choanoflagellata**	–	HM-V*
ns		Chaetonotidae gen. sp.	F h	Obazoa – Opisthokonta – **Metazoa** – Gastrotricha	Guanine	–
ns		Nematoda gen. sp.	F/T h	Obazoa – Opisthokonta – **Metazoa** – Nematoda	Uric acid	–
ns		*Oncorhynchus mykiss* (scale)	F h	Obazoa – Opisthokonta – **Metazoa** – Chordata	Guanine	–
CCF	2912	*Aspergillus nidulans*	F/T h	Obazoa – Opisthokonta – **Fungi** – Ascomycota – Eurotiales	–	MEA
ATCC	SC5314	*Candida albicans*	F/T h	Obazoa – Opisthokonta – **Fungi** – Ascomycota – Saccharomycetales	Guanine	MEA
EUROSCARF	BY4741	*Saccharomyces cerevisiae*	T h	Obazoa – Opisthokonta – **Fungi** – Ascomycota – Saccharomycetales	–	YPAD
CCF	3485	*Neurospora sitophila*	F/T h	Obazoa – Opisthokonta – **Fungi** – Ascomycota – Sordariales	–	MEA
CCVC	CQ1	*Nosema bombycis*	E h p	Obazoa – Opisthokonta – **Opisthosporidia** – **Microsporidia**	–	–
ns		*Woronichinia naegeliana*	F a	Eubacteria – Cyanobacteria	Aerotopes	–
ns		*Oscillatoria* sp.	F a	Eubacteria – Cyanobacteria	Carotenoids, lipids	–
priv		*Bacillus subtilis*	T h	Eubacteria – Firmicutes	–	

617

Table S2. Overview of the Concentrative nucleoside transporter (CNT) distribution among eukaryotes based on HMM search in the database of 57 eukaryotic genomes.

Taxonomic rank	Presence of CNT
Amoebozoa	yes
Holomycota	yes
Chrompodellids	yes
Streptophyta	no
Rhizaria	yes
Stramenopiles	no
Holozoa	yes
Chlorophyta	no
Haptophyta	yes
Cryptophyceae	yes
Apicomplexa	no
Rhodophyta	no
Euglenozoa	no
Metamonada	no
Ciliophora	no
Heterolobosea	no
Perkinsidae	no
Apusomonadida	no

Table S3. Overview of the Equilibrative nucleoside transporter (ENT) distribution among eukaryotes based on HMM search in the database of 57 eukaryotic genomes.

Taxonomic rank	Presence of ENT
Amoebozoa	yes
Holomycota	yes
Chrompodellids	yes
Streptophyta	yes
Rhizaria	yes
Stramenopiles	yes
Holozoa	yes
Chlorophyta	yes
Haptophyta	yes
Cryptophyceae	yes
Apicomplexa	yes
Rhodophyta	yes
Euglenozoa	yes
Metamonada	yes
Ciliophora	yes
Heterolobosea	yes
Perkinsidae	yes
Apusomonadida	yes

Movie S1.

Polarized light microscopy of crystalline inclusions in SAR.

https://youtu.be/cMkMJthq5KQ

Movie S2.

Polarized light microscopy of crystalline inclusions in Haptista, Cryptista and Telonemia.

https://youtu.be/Z30CDbWqOhc

Movie S3.

Polarized light microscopy of crystalline inclusions in Archaeplastida.

https://youtu.be/2ZXfOdpsJcU

Movie S4.

Polarized light microscopy of crystalline inclusions in Amoebozoa.

https://youtu.be/DUbA5e_1_BE

Movie S5.

Polarized light microscopy of crystalline inclusions in Opisthokonta.

https://youtu.be/kyEzbo-IbiM

Movie S6.

Polarized light microscopy of crystalline inclusions in Excavata.

https://youtu.be/XWzNBLmE01A

Movie S7.

Polarized light microscopy of crystalline inclusions in Hemimastigophora.

https://youtu.be/gnUZhZRRfcw

Movie S8.

Polarized light microscopy of crystalline inclusions in Prokaryota – Cyanobacteria.

https://youtu.be/8yGo161rdJU

All the supplementary movies are deposited here: doi: 10.6084/m9.figshare.19604575